

L^1 -STABILITY OF VORTEX SHEETS AND ENTROPY WAVES IN STEADY SUPERSONIC EULER FLOWS OVER LIPSCHITZ WALLS

GUI-QIANG CHEN VAIBHAV KUKREJA

ABSTRACT. We establish the well-posedness of compressible vortex sheets and entropy waves in two-dimensional steady supersonic Euler flows over Lipschitz walls under a BV boundary perturbation. In particular, when the total variation of the incoming flow perturbation around the background strong vortex sheet/entropy wave is small, we prove that the two-dimensional steady supersonic Euler flows containing a strong vortex sheet/entropy wave past a Lipschitz wall are L^1 -stable. Both the Lipschitz wall (whose boundary slope function has small total variation) and incoming flow perturb the background strong vortex sheet/entropy wave. The weak waves are reflected after nonlinear waves interact with the strong vortex sheet/entropy wave and the wall boundary. Using the wave-front tracking method, the existence of solutions in BV over Lipschitz walls is first shown, when the incoming flow perturbation of the background strong vortex sheet/entropy wave has small total variation. Then we establish the L^1 -contraction of the solutions with respect to the incoming flows. To achieve this, a Lyapunov functional, equivalent to the L^1 -distance between two solutions containing strong vortex sheets/entropy waves, is carefully constructed to include the nonlinear waves generated both by the wall boundary and from the incoming flow. This functional is then shown to decrease in the flow direction, leading to the L^1 -stability, as well as the uniqueness, of the solutions. Furthermore, the uniqueness of solutions extends to a larger class of viscosity solutions.

1. INTRODUCTION

We study the well-posedness of two-dimensional steady supersonic Euler flows past a curved Lipschitz wall containing strong vortex sheets/entropy waves in the L^1 -norm. The inviscid compressible flows are governed by the two-dimensional steady Euler system:

$$\begin{cases} (\rho u)_x + (\rho v)_y = 0, \\ (\rho u^2 + p)_x + (\rho uv)_y = 0, \\ (\rho uv)_x + (\rho v^2 + p)_y = 0, \\ (\rho u(E + \frac{p}{\rho}))_x + (\rho v(E + \frac{p}{\rho}))_y = 0, \end{cases} \quad (1.1)$$

with (u, v) , p , ρ , and E representing the fluid velocity, scalar pressure, density, and total energy, respectively. Furthermore, the total energy E is explicitly given by

$$E = \frac{1}{2}(u^2 + v^2) + e(\rho, p),$$

where the internal energy e can be written as a function of (ρ, p) defined through the thermodynamical relations. The temperature T and entropy S are the other two thermodynamic variables.

In the case of an ideal gas, the pressure p and internal energy e can be expressed as

$$p = R\rho T, \quad e = c_\nu T \quad (1.2)$$

with the adiabatic index γ given by

$$\gamma = 1 + \frac{R}{c_\nu} > 1. \quad (1.3)$$

Date: October 15, 2018.

2010 Mathematics Subject Classification. Primary: 35B35, 35B40, 76J20, 35L65, 85A05, 35A05.

Key words and phrases. Full Euler equations, entropy waves, compressible vortex sheets, L^1 -stability, steady flows, supersonic Euler flow, Riemann solutions, Lipschitz wall, BV perturbation, Glimm's functional, nonlinear interaction, global existence.

In particular, in terms of the density ρ and entropy S , we have

$$p = p(\rho, S) = \kappa \rho^\gamma e^{S/c_\nu}, \quad e = \frac{\kappa}{\gamma - 1} \rho^{\gamma-1} e^{S/c_\nu} = \frac{RT}{\gamma - 1}, \quad (1.4)$$

The constants R , c_ν , and κ in the above relations are all greater than zero.

When the entropy $S = \text{constant}$, the flow is called *isentropic*. In this case, the pressure p can be written as a function of the density ρ , $p = p(\rho)$, and the flow is governed by the isentropic Euler equations:

$$\begin{cases} (\rho u)_x + (\rho v)_y = 0, \\ (\rho u^2 + p)_x + (\rho uv)_y = 0, \\ (\rho uv)_x + (\rho v^2 + p)_y = 0. \end{cases} \quad (1.5)$$

Then, by scaling, the pressure-density relation is

$$p(\rho) = \frac{\rho^\gamma}{\gamma}. \quad (1.6)$$

The adiabatic exponent $\gamma > 1$ corresponds to the isentropic polytropic gas. The limiting case $\gamma = 1$ corresponds to the isothermal flow. Define

$$c = \sqrt{p_\rho(\rho, S)}$$

as the sonic speed. For polytropic gases, the sonic speed is $c = \sqrt{\gamma p / \rho}$.

The flow type is classified by the *Mach number* $M = \frac{\sqrt{u^2 + v^2}}{c}$. When $M > 1$, system (1.1) or (1.5) governs a *supersonic* flow (i.e., $u^2 + v^2 > c^2$), which has all real eigenvalues and is hyperbolic. For $M < 1$, system (1.1) or (1.5) governs a *subsonic* flow (i.e., $u^2 + v^2 < c^2$), which has complex eigenvalues and is elliptic-hyperbolic mixed and composite. When $M = 1$, the flow is called *sonic*.

We are interested in whether compressible vortex sheets/entropy waves in supersonic flow over the Lipschitz wall are always stable under the *BV* perturbation of the incoming flow. Multidimensional steady supersonic Euler flows are important in many physical applications (cf. Courant-Friedrichs [11]). In particular, when the upstream flow is a uniform steady flow above the plane wall in $x < 0$ all the time, the flow downstream above a Lipschitz wall in $x > 0$ is governed by a steady Euler flow after a sufficiently long time. Moreover, compressible vortex sheets and entropy waves occur ubiquitously in nature and are fundamental waves. Furthermore, since steady Euler flows are asymptotic states and may be global attractors of the corresponding unsteady Euler flows, it is important to establish the existence of steady Euler flows and understand their qualitative behavior to shed light on the long-time asymptotic behavior of the unsteady compressible Euler flows, one of the most fundamental problems in mathematical fluid dynamics which is still wide open.

We observe that the stability of contact discontinuities for the Cauchy problem for strictly hyperbolic systems in one space dimension under a *BV* perturbation has been studied by Sablé-Tougeron [24] and Corli-Sablé-Tougeron [12]. In particular, the reflection coefficients, such as K_{11} here, are required to be less than one, which is the stability condition for the mixed problem in the strip $\{(t, x) : t \geq 0, -1 < x < 1\}$ in the earlier works; see, e.g., Sablé-Tougeron [24]. Working with the non-isentropic Euler system (1.1) and a uniform upstream flow, Chen-Zhang-Zhu [10] first proved the global existence in *BV* of supersonic Euler flows containing a strong vortex sheet/entropy wave under the *BV* perturbation of the Lipschitz wall by using the Glimm scheme. The essential difference between system (1.1) as analyzed in [10] (and in Sections 2–7 here) and strictly hyperbolic systems as considered in [12, 24] is that two of the four characteristic eigenvalues coincide and have two linearly independent eigenvectors which determine precisely the compressible vortex sheets and entropy waves so that two independent parameters are required to describe them, respectively.

In this paper, for completeness, we first show, via the wave-front tracking method, the existence of solutions to the problem when a small *BV* perturbation is added to the uniform incoming flow. Then the L^1 -stability of entropy solutions containing strong vortex sheets/entropy waves is established. As corollaries of these results, the estimates on the uniformly Lipschitz semigroup \mathfrak{S} of entropy solutions generated by the wave-front tracking approximations are obtained, and the

uniqueness of weak solutions containing strong vortex sheets/entropy waves is established in a larger set of solutions, namely the class of viscosity solutions.

In the following, we focus mainly on the problem in the region Ω over the Lipschitz wall for the supersonic Euler flows $U(u, v, p, \rho)$ governed by system (1.1), given that the corresponding problem for the isentropic system (1.5) is simpler to analyze. The subsequent figure provides the schematic diagram for the problem we study:

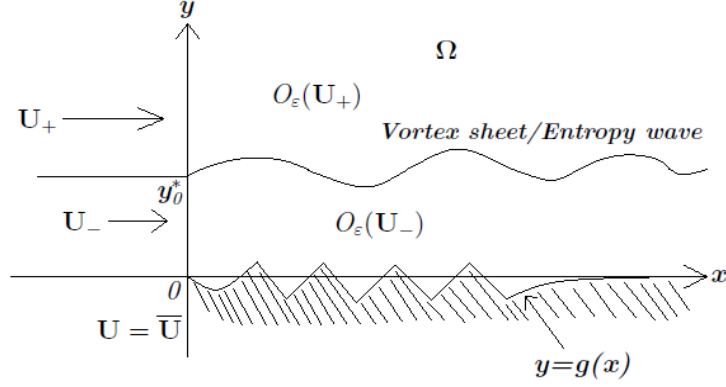


FIGURE 1.1. Stability of the compressible vortex sheet/entropy wave in supersonic flow

The boundary and initial data in the problem are as follows:

- (i) There is a Lipschitz function $g \in \text{Lip}(\mathbb{R}_+; \mathbb{R})$ such that

$$g(0) = g'(0+) = 0, \quad \lim_{x \rightarrow \infty} \arctan(g'(x+)) = 0, \quad g' \in BV(\mathbb{R}_+; \mathbb{R})$$

and

$$\text{TV}(g'(\cdot)) < \varepsilon \quad \text{for some constant } \varepsilon > 0.$$

Denote $\Omega := \{(x, y) : y > g(x), x \geq 0\}$, $\Gamma := \{(x, y) : y = g(x), x \geq 0\}$, and $\mathbf{n}(x\pm) = \frac{(-g'(x\pm), 1)}{\sqrt{(g'(x\pm))^2 + 1}}$ as the outer normal vectors to Γ at the respective points $x\pm$ (cf. Fig. 1.1).

- (ii) The incoming flow $U = \bar{U}(y) := U_0^b + \tilde{U}_0$ at $x = 0$ is composed of two parts:
- (a) The upstream flow U_0^b consists of one straight vortex sheet/entropy wave $y = y_0^* > 0$ and two constant vectors $U_0^- = U_-$, when $0 < y < y_0^*$, and $U_0^+ = U_+$, when $y > y_0^* > 0$, satisfying

$$v_- = v_+ = 0, \quad u_{\pm} > c_{\pm} > 0,$$

where $c_{\pm} = \sqrt{\gamma p_{\pm} / \rho_{\pm}}$ is the sonic speed of state U_{\pm} .

- (b) The BV perturbation $\tilde{U}_0 = (\tilde{u}_0, \tilde{v}_0, \tilde{p}_0, \tilde{\rho}_0)(y) \in L^1 \cap BV(\mathbb{R}; \mathbb{R}^4)$ at $x = 0$ so that $\text{TV}(\tilde{U}_0) \ll 1$.

Then we consider the following initial-boundary value problem for system (1.1):

$$\text{Cauchy Condition :} \quad U|_{x=0} = \bar{U}(y) = U_0^b + \tilde{U}_0; \quad (1.7)$$

$$\text{Boundary Condition :} \quad (u, v) \cdot \mathbf{n} = 0 \quad \text{on } \Gamma. \quad (1.8)$$

Definition 1.1 (*Admissible entropy solutions*). A BV function $U = U(x, y)$ is said to be an entropy solution of the initial-boundary value problem (1.1) and (1.7)–(1.8) if and only if the following conditions hold:

- (i) U is a weak solution of (2.1) and satisfies

$$U|_{x=0} = \bar{U}(y) \quad \text{and} \quad (u, v) \cdot \mathbf{n}|_{y=g(x)} = 0 \quad \text{in the trace sense;}$$

- (ii) U satisfies the *steady entropy Clausius inequality*:

$$(\rho u S)_x + (\rho v S)_y \geq 0 \quad (1.9)$$

in the distributional sense in Ω including the Lipschitz wall boundary.

One of the essential developments within this paper is to develop suitable methods to deal with the challenges caused by the nonstrictly hyperbolicity of the system and the Lipschitz wall boundary, in comparison with the previous progress with the strictly hyperbolic systems of conservation laws, particularly to the analysis of the Cauchy problem. For supersonic Euler flow with a strong shock-front emanating from the wedge vertex, Chen-Li [9] worked out the issue for a Lipschitz wedge boundary. We now discuss some main differences in our work here from the Cauchy problem and the resulting key difficulties. We remark that, in the case of the Cauchy problem concerning only *weak* waves, the decrease of the Lyapunov functional and the L^1 -stability of the solutions were obtained through the cancellation of distances on both sides of waves. In the presence of a strong shock, for the L^1 -stability of solutions of the Cauchy problem for strictly hyperbolic systems of conservation laws, the Lyapunov functional was found to decrease by employing the strength of the strong shock to control the strengths of weak waves of the other families (e.g., see Lewicka-Trivisa [21]). In contrast with our Lipschitz wall problem, which is a problem of initial-boundary value type, there is no such cancellation by the boundary as only one-side is possible near it. Furthermore, no strong vortex sheets/entropy waves (characteristic discontinuities) nor strong shocks are present to handle the strength of the weak waves of the other families, and the terms in the estimates for the first and fourth family carry different signs. As such, it is difficult to say whether the functional can be made to decrease for our case of strong vortex sheets and entropy waves with multiplicity of eigenvalues. One of the key steps to resolve this is to use the physical feature of the boundary condition that the flow of two solutions near the boundary must run in parallel (also see [9]). This observation helps us to obtain additional quantitative relations near the boundary. Then, applying suitable weights and adjustments in the coefficients of the Lyapunov functional and using the cancellation between the different families, the functional is found to decrease in the flow direction.

The rest of the paper is organized as follows. In Section 2, we recall some fundamental properties of the two-dimensional steady Euler system (1.1) and discuss related nonlinear waves and wave interaction estimates. In Section 3, the wave-front tracking algorithm is discussed, working in the presence of strong vortex sheets/entropy waves, the suitable interaction potential \mathcal{Q} is constructed, including the effect of the Lipschitz wall, and the existence of entropy solutions in BV is established for the initial-boundary value problem. In Section 4, we construct the Lyapunov functional Φ (equivalent to the L^1 -distance between two entropy solutions U and V) to include the nonlinear waves produced by the wall boundary vertices. Then, in Section 5, the monotone decrease of the functional Φ is established in the flow direction, leading to the L^1 -stability of the solutions containing strong vortex sheets/entropy waves. Using the estimates established in Sections 3–5, in Section 6, we obtain the existence of a Lipschitz semigroup of solutions generated by a wave-front tracking approximation, as well as some estimates on the uniformly Lipschitz semigroup \mathcal{S} produced by the limit of wave-front tracking approximations. Moreover, the uniqueness of solutions with strong vortex sheets/entropy waves is obtained in the larger class of viscosity solutions.

2. ADIABATIC EULER EQUATIONS: NONLINEAR WAVES AND WAVE INTERACTIONS

In this section, we first present some basic properties of the steady Euler system (1.1). Then related nonlinear waves and interaction estimates are discussed, which will be employed in the later sections.

Consider the following vector functions of the solution U :

$$W(U) = (\rho u, \rho u^2 + p, \rho uv, \rho u(h + \frac{u^2 + v^2}{2}))^\top,$$

$$H(U) = (\rho v, \rho uv, \rho v^2 + p, \rho v(h + \frac{u^2 + v^2}{2}))^\top,$$

where $h = \frac{\gamma p}{(\gamma-1)\rho}$. Then the steady Euler equations in (1.1) can be expressed in the following conservative form:

$$W(U)_x + H(U)_y = 0, \quad U = (u, v, p, \rho)^\top \tag{2.1}$$

When $U(x, y)$ is a smooth solution, system (2.1) is equivalent to

$$\nabla_U W(U)U_x + \nabla_U H(U)U_y = 0. \quad (2.2)$$

Then the roots of the fourth degree polynomial

$$\det(\lambda \nabla_U W(U) - \nabla_U H(U)), \quad (2.3)$$

are the eigenvalues of (2.1); that is, the solutions of the equation

$$(v - \lambda u)^2((v - \lambda u)^2 - c^2(1 + \lambda^2)) = 0, \quad (2.4)$$

where $c = \sqrt{\frac{\gamma p}{\rho}}$ is the sonic speed. For supersonic flows (i.e. $u^2 + v^2 > c^2$), system (2.1) is hyperbolic. Specifically, when $u > c$, system (2.1) has four real eigenvalues in the x -direction:

$$\begin{aligned} \lambda_d &= \frac{uv + (-1)^d c \sqrt{u^2 + v^2 - c^2}}{u^2 - c^2}, & d = 1, 4; \\ \lambda_k &= \frac{v}{u}, & k = 2, 3, \end{aligned} \quad (2.5)$$

with the four corresponding linearly independent eigenvectors given by

$$\begin{aligned} \mathbf{r}_d &= \kappa_d(-\lambda_d, 1, \rho(\lambda_d u - v), \frac{\rho(\lambda_d u - v)}{c^2})^\top, & d = 1, 4, \\ \mathbf{r}_2 &= (u, v, 0, 0)^\top, & \mathbf{r}_3 = (0, 0, 0, \rho)^\top, \end{aligned} \quad (2.6)$$

where κ_d the re-normalization factors such that $\mathbf{r}_d \cdot \nabla \lambda_d = 1$, given that the d th-characteristic fields, $d = 1, 4$, are genuinely nonlinear. The second and third linearly degenerate characteristic fields satisfy $\mathbf{r}_k \cdot \nabla \lambda_k = 0$, $k = 2, 3$, which correspond to vortex sheets and entropy waves, respectively.

The wave curves in the phase space are now described. The Rankine-Hugoniot jump conditions for (2.1) are

$$\sigma [W(u)] = [H(u)], \quad (2.7)$$

and the discontinuity propagates with the speed σ .

There are two different waves associated with the fields $\lambda_k = \frac{v_0}{u_0}$, $k = 2, 3$, with the corresponding linearly independent right eigenvectors \mathbf{r}_k , $k = 2, 3$, in (2.6):

Vortex sheets:

$$C_2(U_0) : \quad \sigma = \frac{v}{u} = \frac{v_0}{u_0}, \quad p = p_0, \quad S = S_0, \quad u^2 + v^2 \neq u_0^2 + v_0^2, \quad (2.8)$$

Entropy waves:

$$C_3(U_0) : \quad \sigma = \frac{v}{u} = \frac{v_0}{u_0}, \quad p = p_0, \quad (u, v) = (u_0, v_0), \quad S \neq S_0. \quad (2.9)$$

Albeit the two contact discontinuities, the vortex sheet and the entropy wave, above match as a single discontinuity in the physical (x, y) -plane, two independent parameters are needed to describe them in the phase space $U = (u, v, p, \rho)$ since there are two linearly independent eigenvectors corresponding to the repeated eigenvalues $\lambda_2 = \lambda_3 = \frac{v}{u}$ of the linearly degenerate characteristics fields.

The nonlinear waves associated with λ_d , $d = 1, 4$, are shock waves and rarefaction waves. The shock waves have their speeds of propagation given by

$$\sigma = \sigma_d := \frac{u_0 v_0 + (-1)^d \bar{c}_0 \sqrt{u_0^2 + v_0^2 - \bar{c}_0^2}}{u^2 - \bar{c}_0^2}, \quad d = 1, 4,$$

where $\bar{c}_0^2 = \frac{c_0^2}{b_0} \frac{\rho}{\rho_0}$ and $b_0 = \frac{\gamma+1}{2} - \frac{\gamma-1}{2} \frac{\rho}{\rho_0}$. Substituting σ_d , $d = 1, 4$, into (2.7), the d -Hugoniot curve $S_d(U_0)$ through the state U_0 is

$$S_d(U_0) : \quad [p] = \frac{c_0^2}{b_0} [\rho], \quad [u] = -\sigma_d [v], \quad \rho_0(\sigma_d u_0 - v_0)[v] = [p], \quad d = 1, 4.$$

Written as $S_d^+(U_0)$, $d = 1, 4$, the half curves of $S_d(U_0)$ for $\rho > \rho_0$ in the phase space are said to be the shock curves on which any state forms a shock with the below state U_0 in the (x, y) -plane

respecting the entropy condition (1.9). Furthermore, for each $d = 1$ or $d = 4$, the curves $S_d^+(U_0)$ and $R_d^-(U_0)$ at the state U_0 have the same curvature.

If U is a piecewise smooth solution (see also [10]), then any of the following conditions below is equivalent to the entropy inequality (1.9) in Definition 1.1 for a shock wave:

(i) *The physical entropy condition:* The density increases across the shock in the flow direction,

$$\rho_{\text{back}} < \rho_{\text{front}}. \quad (2.10)$$

(ii) *The Lax entropy condition:* On the d th-shock, the shock speed σ_d satisfies

$$\lambda_d(\text{back}) < \sigma_d < \lambda_d(\text{front}) \quad \text{for } d = 1, 4, \quad (2.11)$$

$$\sigma_1 < \lambda_{2,3}(\text{back}), \quad \lambda_{2,3}(\text{front}) < \sigma_4. \quad (2.12)$$

The rarefaction wave curves $R_l^-(U_0)$ through the state U_0 in the state space are given by

$$R_d^- : \quad dp = c^2 d\rho, \quad du = -\lambda_d dv, \quad \rho(\lambda_d u - v)dv = dp \quad \text{for } \rho < \rho_0, \quad d = 1, 4. \quad (2.13)$$

We next discuss several essential properties of the nonlinear waves and related wave interaction estimates in Lemmas 2.1–2.7 below. These facts will be used in the later sections. We also refer the reader to Chen-Zhang-Zhu [10] for further details.

2.1. Riemann Problems and Riemann Solutions

We focus on the related Riemann problems and their solutions in this section, which serve as the building blocks for the front tracking algorithm for the initial-boundary value problem (2.1) and (1.7)–(1.8).

Riemann problem of lateral-type. We note that the *straight-sided wall problem* is the case when problem (2.1) and (1.7)–(1.8) is considered with the boundary $g \equiv 0$. It can be seen that, when the angle between the straight-sided wall and the flow direction of the incoming flow is zero, problem (2.1) and (1.7)–(1.8) has an entropy solution made up of two constant states $U_- = (u_-, 0, p_-, \rho_-)$ and $U_+ = (u_+, 0, p_+, \rho_+)$, satisfying $u_{\pm} > c_{\pm} > 0$ in the subdomains Ω_+ and Ω_- of Ω separated by a straight vortex sheet/entropy wave. These are precisely the states U_- and U_+ below and above the large vortex sheet/entropy wave. The principal aim of this paper is to establish the L^1 -well-posedness for problem (2.1) and (1.7)–(1.8) for the solutions near the background solution containing a strong vortex sheet/entropy wave $\{U_-, U_+\}$ with $g \equiv 0$.

It has been observed in [11] that, if the angle between the flow direction of the front state and the wall at a boundary vertex is smaller than π and larger than the extreme angle determined by the incoming flow state and $\gamma \geq 1$, then a unique 4-shock is generated, separating the front-state from the supersonic back-state. If the angle between the flow direction of the front-state and the wall at a boundary vertex is larger than π and less than the extreme angle, then a 4-rarefaction wave is produced, emanating from the vertex. These waves are easily seen through the shock polar analysis (cf. [10, 11]). This signifies that, when the angle between the flow direction of the front-state and the wall at a boundary vertex is close to π , the lateral Riemann problem can be uniquely solved. For further details, see Lemma 2.3 and [10]. For an indepth discussion, we also refer to Courant–Friedrichs [11].

Riemann problem involving only weak waves. Consider the subsequent initial value problem with piecewise constant initial data:

$$\begin{cases} W(U)_x + H(U)_y = 0, \\ U|_{x=x_0} = \underline{U} = \begin{cases} U_a, & y > y_0, \\ U_b, & y < y_0, \end{cases} \end{cases} \quad (2.14)$$

with the constant states U_a and U_b denoting the *above* state and *below* state with respect to the line $y = y_0$, respectively. Then there is $\varepsilon > 0$ so that, for any states U_b, U_a in the neighborhood $O_\varepsilon(U_+)$ of U_+ , or U_b, U_a in the neighborhood $O_\varepsilon(U_-)$ of U_- , the initial value problem (2.14) has a

unique admissible solution consisting of four waves, consisting of shocks, rarefaction waves, vortex sheets and/or entropy waves.

Riemann problem involving the strong vortex sheets/entropy waves. From now on, the notation $\{U_b, U_a\} = (\alpha_1, \alpha_2, \alpha_3, \alpha_4)$ will be used to write $U_a = \Phi(\alpha_4, \alpha_3, \alpha_2, \alpha_1; U_b)$ as the solution of the Riemann problem, where $\Phi \in C^2$, and α_j is the strength of the j -wave. For any wave with $U_b \in O_\varepsilon(U_-)$ and $U_a \in O_\varepsilon(U_+)$, we also use $\{U_b, U_a\} = (0, \sigma_2, \sigma_3, 0)$ to denote the strong vortex sheet/entropy wave that connects U_b and U_a with strength (σ_2, σ_3) . That is,

$$U_m = \Phi(\sigma_2; U_b) := (u_b e^{\sigma_2}, v_b e^{\sigma_2}, p_b, \rho_b), \quad U_a = \Phi(\sigma_3; U_m) := (u_m, v_m, p_m, \rho_m e^{\sigma_3}).$$

Particularly, we observe that

$$U_+ = (u_+, 0, p_+, \rho_+) = (u_- e^{\sigma_{20}}, 0, p_-, \rho_- e^{\sigma_{30}}).$$

We write $G(\sigma_3, \sigma_2; U_b) = \Phi_3(\sigma_3; \Phi_2(\sigma_2; U_b))$ for any $U_b \in O_\varepsilon(U_-)$. Then we have

Lemma 2.1. *The vector function $G(\sigma_3, \sigma_2; U_b)$ satisfies*

$$G_{\sigma_2}(\sigma_3, \sigma_2; U_b) = (u_b e^{\sigma_2}, v_b e^{\sigma_2}, 0, 0), \quad G_{\sigma_3}(\sigma_3, \sigma_2; U_b) = (0, 0, 0, \rho_b e^{\sigma_3}), \quad (2.15)$$

and

$$\nabla_U G(\sigma_3, \sigma_2; U_b) = \text{diag}(e^{\sigma_2}, e^{\sigma_2}, 1, e^{\sigma_3}). \quad (2.16)$$

Furthermore, for the plane vortex sheet and entropy wave with the lower state $U_- = (u_-, 0, p_-, \rho_-)$, upper state $U_+ = (u_+, 0, p_+, \rho_+)$, and strength $(\sigma_{20}, \sigma_{30})$,

$$\det(\mathbf{r}_4(U_+), G_{\sigma_3}(\sigma_{30}, \sigma_{20}; U_-), G_{\sigma_2}(\sigma_{30}, \sigma_{20}; U_-), \nabla_U G(\sigma_{30}, \sigma_{20}; U_-) \cdot \mathbf{r}_1(U_-)) > 0. \quad (2.17)$$

These can be easily obtained from direct calculations and are thus omitted.

The properties in (2.15)–(2.17) above play a fundamental role in achieving the necessary estimates on the strengths of reflected weak waves in the interaction between the strong vortex sheet/entropy wave and weak waves (see the proofs for Lemmas 2.4–2.7).

2.2. Wave Interactions and Reflection Estimates. In the following, several essential estimates are provided on wave interactions and reflections. For their proofs and all the related details, we refer to [10].

Weak wave interactions estimates. For the weak wave interaction away from both the strong vortex sheet/entropy wave and the wall boundary in the regions Ω_+ or Ω_- , we have the following estimate:

Lemma 2.2. *Assume that*

$$U_b, U_m, U_a \in O_\varepsilon(U_+), \quad \text{or} \quad U_b, U_m, U_a \in O_\varepsilon(U_-),$$

are three states with $\{U_b, U_m\} = (\alpha_1, \alpha_2, \alpha_3, \alpha_4)$, $\{U_m, U_a\} = (\beta_1, \beta_2, \beta_3, \beta_4)$. Then $\{U_b, U_a\} = (\gamma_1, \gamma_2, \gamma_3, \gamma_4)$ with

$$\gamma_i = \alpha_i + \beta_i + O(1)\Delta(\alpha, \beta), \quad (2.18)$$

where $\Delta(\alpha, \beta) = (|\alpha_4| + |\alpha_3| + |\alpha_2|)|\beta_1| + |\alpha_4|(|\beta_2| + |\beta_3|) + \sum_{j=1,4} \Delta_j(\alpha, \beta)$ and

$$\Delta_j(\alpha, \beta) = \begin{cases} 0, & \alpha_j \geq 0, \beta_j \geq 0, \\ |\alpha_j||\beta_j|, & \text{otherwise.} \end{cases} \quad (2.19)$$

Estimates on the boundary perturbation of weak waves and the reflection of weak waves on the boundary. We write $\{C_l(a_l, b_l)\}_{l=0}^\infty$ for the points $\{(a_l, b_l)\}_{l=0}^\infty$ in the (x, y) -plane with $0 < a_l < a_{l+1}$. Define

$$\begin{cases} \theta_{l,l+1} = \arctan\left(\frac{b_{l+1}-b_l}{a_{l+1}-a_l}\right), \quad \theta_l = \theta_{l,l+1} - \theta_{l-1,l}, \quad \theta_{-1,0} = 0, \\ \Omega_{l+1} = \{(x, y) : x \in [a_l, a_{l+1}], y > b_l + (x - a_l)\tan(\theta_{l,l+1})\}, \\ \Gamma_{l+1} = \{(x, y) : x \in (a_l, a_{l+1}), y = b_l + (x - a_l)\tan(\theta_{l,l+1})\}, \end{cases} \quad (2.20)$$

and the outer normal vector to Γ_l :

$$\mathbf{n}_{l+1} = \frac{(b_{l+1} - b_l, a_l - a_{l+1})}{\sqrt{(b_{l+1} - b_l)^2 + (a_{l+1} - a_l)^2}} = (\sin(\theta_l, \theta_{l+1}), -\cos(\theta_l, \theta_{l+1})). \quad (2.21)$$

With the constant state \underline{U} , consider the following initial-boundary value problem:

$$\begin{cases} (2.1) & \text{in } \Omega_{l+1}, \\ U|_{x=a_l} = \underline{U}, \\ (u, v) \cdot \mathbf{n}_{l+1} = 0 & \text{on } \Gamma_{l+1}. \end{cases} \quad (2.22)$$

Lemma 2.3. *Suppose $\{U_m, U_a\} = (\beta_1, \beta_2, \beta_3, 0)$ and $\{U_l, U_m\} = (0, 0, 0, \alpha_4)$ with*

$$(u_l, v_l) \cdot \mathbf{n}_l = 0.$$

Then there exists a unique solution U_{l+1} of problem (2.22) such that $\{U_{l+1}, U_a\} = (0, 0, 0, \delta_4)$ and $U_{l+1} \cdot (\mathbf{n}_{l+1}, 0, 0) = 0$. Moreover,

$$\delta_4 = \alpha_4 + K_{b1}\beta_1 + K_{b2}\beta_2 + K_{b3}\beta_3 + K_{b0}\theta_l, \quad (2.23)$$

where K_{b1}, K_{b2}, K_{b3} , and K_{b0} are C^2 -functions of $\beta_3, \beta_2, \beta_1, \alpha_4, \theta_{l+1}$, and U_a satisfying

$$K_{b1}|_{\{\theta_l=\alpha_4=\beta_1=\beta_2=\beta_3=0, U_a=U_-\}} = 1, \quad K_{bi}|_{\{\theta_l=\alpha_4=\beta_1=\beta_2=\beta_3=0, U_a=U_-\}} = 0, \quad i = 2, 3, \quad (2.24)$$

and K_{b0} is bounded. In particular, $K_{b0} < 0$ at the origin.

This lemma has two purposes. The first is to estimate the weak waves generated by the vertices on the Lipschitz wall boundary. This boundedness will be used to control the boundary perturbation; see (3.2) in the construction of the wave interaction potential $\mathcal{Q}(x)$. The second is to estimate the strength of the reflected wave δ_4 with respect to the incident wave α_1 . Property (2.24) of the coefficients will play an important role to control the reflected waves.

Estimates on the interaction between the strong vortex sheet/entropy wave and weak waves from below. Estimate (2.25) below plays a key role in ensuring the L^1 -stability of entropy solutions, especially for the existence of the constants w_1^b and w_4^b in Lemma 5.1 (see below). This estimate also ensures the existence of $K^* \in (K_{11}, 1)$ in the construction of the wave interaction potential $\mathcal{Q}(x)$ in (3.2).

Lemma 2.4. *Let $U_b, U_m \in O_\varepsilon(U_-)$ and $U_a \in O_\varepsilon(U_+)$ with*

$$\{U_b, U_m\} = (0, \alpha_2, \alpha_3, \alpha_4), \quad \{U_m, U_a\} = (\beta_1, \sigma_2, \sigma_3, 0).$$

Then there exists a unique $(\delta_1, \sigma_2', \sigma_3', \delta_4)$ such that the Riemann problem (2.14) admits an admissible solution that consists of a weak 1-wave of strength δ_1 , a strong vortex sheet of strength σ_2 , a strong entropy wave of strength σ_3 , and a weak 4-wave of strength δ_4 :

$$\{U_b, U_a\} = (\delta_1, \sigma_2', \sigma_3', \delta_4).$$

Moreover,

$$\begin{aligned} \delta_1 &= \beta_1 + K_{11}\alpha_4 + O(1)\Delta', & \delta_4 &= K_{14}\alpha_4 + O(1)\Delta', \\ \sigma_2' &= \sigma_2 + \alpha_2 + K_{12}\alpha_4 + O(1)\Delta', & \sigma_3' &= \sigma_3 + \alpha_3 + K_{13}\alpha_4 + O(1)\Delta', \\ |K_{11}|_{\{\alpha_4=\alpha_3=\alpha_2=0, \sigma_2'=\sigma_{20}, \sigma_3'=\sigma_{30}\}} &= \left| \frac{\lambda_4(U_+)e^{2\sigma_{20}+\sigma_{30}} - \lambda_4(U_-)}{\lambda_4(U_+)e^{2\sigma_{20}+\sigma_{30}} + \lambda_4(U_-)} \right| < 1, \end{aligned} \quad (2.25)$$

where $\Delta' = |\beta_1|(|\alpha_2| + |\alpha_3|)$, and $\sum_{j=2}^4 |K_{1j}|$ is bounded.

Lemma 2.5. *The coefficient $|K_{14}|_{\{\alpha_4=\alpha_3=\alpha_2=0, \sigma_2'=\sigma_{20}, \sigma_3'=\sigma_{30}\}}$ in the strength δ_4 of a weak 4-wave in Lemma 2.4 remains bounded away from zero.*

Proof. By Lemma 2.4, we can find a unique solution $(\delta_1, \sigma_2', \sigma_3', \delta_4)$ as a C^2 -function of $\alpha_2, \alpha_3, \alpha_4, \beta_1, \sigma_2, \sigma_3$, and U_b to

$$\Phi_4(\delta_4; G(\sigma_3', \sigma_2'; \Phi_1(\delta; U_b))) = G(\sigma_2, \sigma_3; \Phi_1(\beta_1, \Phi(\alpha_4, \alpha_3, \alpha_2, 0; U_b))). \quad (2.26)$$

That is,

$$\sigma'_i = \sigma'_i(\alpha_2, \alpha_3, \alpha_4, \beta_1, \sigma_2, \sigma_3), \quad i = 2, 3; \quad \delta_j = \delta_j(\alpha_2, \alpha_3, \alpha_4, \beta_1, \sigma_2, \sigma_3), \quad j = 1, 4,$$

where we have omitted U_b for simplicity.

From [10], we know that

$$K_{1j} = \int_0^1 \partial_{\alpha_4} \delta_j(\alpha_2, \alpha_3, \theta \alpha_4, \beta_1, \sigma_2, \sigma_3) d\theta, \quad j = 1, 4.$$

Differentiate (2.26) with respect to α_4 , and let $\beta_1 = \alpha_4 = \alpha_3 = \alpha_2 = 0, \sigma_2 = \sigma_{20}$, and $\sigma_3 = \sigma_{30}$. We obtain

$$\begin{aligned} \nabla_U G(\sigma_{30}, \sigma_{20}; U_-) \cdot \mathbf{r}_4(U_-) &= \partial_{\alpha_4} \delta_4 \mathbf{r}_4(U_+) + \partial_{\alpha_4} \sigma'_3 G_{\sigma_3}(\sigma_{30}, \sigma_{20}; U_-) \\ &\quad + \partial_{\alpha_4} \sigma'_2 G_{\sigma_2}(\sigma_{30}, \sigma_{20}; U_-) + \partial_{\alpha_4} \delta_1 \nabla_U G(\sigma_{30}, \sigma_{20}; U_-) \cdot \mathbf{r}_1(U_-). \end{aligned}$$

By Lemma 2.1, we have

$$\begin{aligned} &|\partial_{\alpha_4} \delta_4| \\ &= \left| \frac{\det(\nabla_U G(\sigma_{30}, \sigma_{20}; U_-) \cdot \mathbf{r}_4(U_-), G_{\sigma_3}(\sigma_{30}, \sigma_{20}; U_-), G_{\sigma_2}(\sigma_{30}, \sigma_{20}; U_-), \nabla_U G(\sigma_{30}, \sigma_{20}; U_-) \cdot \mathbf{r}_1(U_-))}{\det(\mathbf{r}_4(U_+), G_{\sigma_3}(\sigma_{30}, \sigma_{20}; U_-), G_{\sigma_2}(\sigma_{30}, \sigma_{20}; U_-), \nabla_U G(\sigma_{30}, \sigma_{20}; U_-) \cdot \mathbf{r}_1(U_-))} \right| \\ &= \left| \frac{\kappa_1(U_-) \kappa_4(U_-) \rho_-^2 u_-^2 e^{2\sigma_{20} + \sigma_{30}} (\lambda_4(U_-) - \lambda_1(U_-))}{\kappa_1(U_-) \kappa_4(U_+) \rho_+^2 u_+^2 e^{2\sigma_{20} + \sigma_{30}} (\lambda_4(U_+) e^{2\sigma_{20} + \sigma_{30}} - \lambda_1(U_-))} \right| \\ &= \left| \frac{2\kappa_4(U_-) e^{\sigma_{20}} \lambda_4(U_-)}{\kappa_4(U_+) (\lambda_4(U_+) e^{2\sigma_{20} + \sigma_{30}} + \lambda_4(U_-))} \right| > 0. \end{aligned}$$

This completes the proof.

Estimates on the interaction between the strong vortex sheet/entropy wave and weak waves from above. We have

Lemma 2.6. *Let $U_b \in O_\varepsilon(U_-)$ and $U_m, U_a \in O_\varepsilon(U_+)$ with*

$$\{U_b, U_m\} = (0, \sigma_2, \sigma_3, \alpha_4), \quad \{U_m, U_a\} = (\beta_1, \beta_2, \beta_3, 0).$$

Then there exists a unique $(\delta_1, \sigma'_2, \sigma'_3, \delta_4)$ such that the Riemann problem (2.14) admits an admissible solution that consists of a weak 1-wave of strength δ_1 , a strong vortex sheet of strength σ_2 , a strong entropy wave of strength σ_3 , and a weak 4-wave of strength δ_4 :

$$\{U_b, U_a\} = (\delta_1, \sigma'_2, \sigma'_3, \delta_4).$$

Moreover,

$$\begin{aligned} \delta_1 &= K_{21} \beta_1 + O(1) \Delta'', \quad \sigma'_2 = \sigma_2 + \beta_2 + K_{22} \beta_1 + O(1) \Delta'', \\ \sigma'_3 &= \sigma_3 + \beta_3 + K_{23} \beta_1 + O(1) \Delta'', \quad \delta_4 = \alpha_4 + K_{24} \beta_1 + O(1) \Delta'', \end{aligned}$$

where $\sum_{j=1}^4 |K_{2j}|$ is bounded and $\Delta'' = |\alpha_4|(|\beta_2| + |\beta_3|)$.

The constant K_{21} here is used in the definition of weighted strength b_α of weak waves in (3.1).

Lemma 2.7. *The coefficient $|K_{21}|_{\{\beta_3=\beta_2=\beta_1=0, \sigma'_2=\sigma_{20}, \sigma'_3=\sigma_{30}\}}$ in the strength δ_1 of a weak 1-wave in Lemma 2.6 remains bounded away from zero, while the reflection coefficient $|K_{24}| < 1$.*

Proof. By Lemma 2.6, we can find a unique solution $(\delta_1, \sigma'_2, \sigma'_3, \delta_4)$ as a C^2 -function of $\alpha_2, \alpha_3, \alpha_4, \beta_1, \sigma_2, \sigma_3$, and U_b to

$$\Phi_4(\delta_4; G(\sigma'_3, \sigma'_2; \Phi_1(\delta; U_b))) = \Phi(0, \beta_3, \beta_2, \beta_1; \Phi_4(\alpha_4; G(\sigma_3, \sigma_2; U_b))). \quad (2.27)$$

That is,

$$\sigma'_i = \sigma'_i(\beta_1, \beta_2, \beta_3, \alpha_4, \sigma_2, \sigma_3), \quad i = 2, 3; \quad \delta_j = \delta_j(\beta_1, \beta_2, \beta_3, \alpha_4, \sigma_2, \sigma_3), \quad j = 1, 4,$$

where we have omitted U_b for simplicity.

From [10], we know that

$$K_{2j} = \int_0^1 \partial_{\beta_1} \partial_j (\theta \beta_1, \beta_2, \beta_3, \alpha_4, \sigma_2, \sigma_3) d\theta, \quad j = 1, 4.$$

Differentiate (2.27) with respect to β_1 and let $\alpha_4 = \beta_1 = \beta_2 = \beta_3 = 0$, $\sigma_2 = \sigma_{20}$, and $\sigma_3 = \sigma_{30}$. We obtain

$$\begin{aligned} \mathbf{r}_1(U_+) &= \partial_{\beta_1} \delta_4 \mathbf{r}_4(U_+) + \partial_{\beta_1} \sigma_3' G_{\sigma_3}(\sigma_{30}, \sigma_{20}; U_-) \\ &\quad + \partial_{\beta_1} \sigma_2' G_{\sigma_2}(\sigma_{30}, \sigma_{20}; U_-) + \partial_{\beta_1} \delta_1 \nabla_U G(\sigma_{30}, \sigma_{20}; U_-) \cdot \mathbf{r}_1(U_-). \end{aligned}$$

By Lemma 2.1, we have

$$\begin{aligned} |\partial_{\beta_1} \delta_1| &= \left| \frac{\det(\mathbf{r}_4(U_+), G_{\sigma_3}(\sigma_{30}, \sigma_{20}; U_-), G_{\sigma_2}(\sigma_{30}, \sigma_{20}; U_-), \mathbf{r}_1(U_+))}{\det(\mathbf{r}_4(U_+), G_{\sigma_3}(\sigma_{30}, \sigma_{20}; U_-), G_{\sigma_2}(\sigma_{30}, \sigma_{20}; U_-), \nabla_U G(\sigma_{30}, \sigma_{20}; U_-) \cdot \mathbf{r}_1(U_-))} \right| \\ &= \left| \frac{\kappa_4(U_+) \kappa_1(U_+) \rho_-^2 u_-^2 e^{\sigma_{20} + \sigma_{30}} (\lambda_4(U_+) e^{\sigma_{20} + \sigma_{30}} - \lambda_1(U_+) e^{\sigma_{20} + \sigma_{30}})}{\kappa_4(U_+) \kappa_1(U_-) \rho_-^2 u_-^2 e^{\sigma_{20} + \sigma_{30}} (\lambda_4(U_+) e^{2\sigma_{20} + \sigma_{30}} - \lambda_1(U_-))} \right| \\ &= \left| \frac{2\kappa_1(U_+) \lambda_4(U_+) e^{\sigma_{20} + \sigma_{30}}}{\kappa_1(U_-) (\lambda_4(U_+) e^{2\sigma_{20} + \sigma_{30}} + \lambda_4(U_-))} \right| > 0. \end{aligned}$$

However, for the reflection coefficient $|K_{24}|$, we have

$$\begin{aligned} |\partial_{\beta_1} \delta_4| &= \left| \frac{\det(\mathbf{r}_1(U_+), G_{\sigma_3}(\sigma_{30}, \sigma_{20}; U_-), G_{\sigma_2}(\sigma_{30}, \sigma_{20}; U_-), \nabla_U G(\sigma_{30}, \sigma_{20}; U_-) \cdot \mathbf{r}_1(U_-))}{\det(\mathbf{r}_4(U_+), G_{\sigma_3}(\sigma_{30}, \sigma_{20}; U_-), G_{\sigma_2}(\sigma_{30}, \sigma_{20}; U_-), \nabla_U G(\sigma_{30}, \sigma_{20}; U_-) \cdot \mathbf{r}_1(U_-))} \right| \\ &= \left| \frac{\kappa_1(U_-) \kappa_1(U_+) \rho_- u_- e^{\sigma_{20} + \sigma_{30}} (-\rho_- u_- \lambda_1(U_-) + e^{\sigma_{20}} \rho_+ u_+ \lambda_1(U_+))}{\kappa_4(U_+) \kappa_1(U_-) \rho_-^2 u_-^2 e^{\sigma_{20} + \sigma_{30}} (\lambda_4(U_+) e^{2\sigma_{20} + \sigma_{30}} - \lambda_1(U_-))} \right| \\ &= \left| \frac{-\lambda_4(U_+) e^{2\sigma_{20} + \sigma_{30}} + \lambda_4(U_-)}{\lambda_4(U_+) e^{2\sigma_{20} + \sigma_{30}} + \lambda_4(U_-)} \right| < 1, \end{aligned}$$

where $|K_{24}|$ is not necessarily bounded away from zero, but is less than one.

3. THE WAVE-FRONT TRACKING ALGORITHM AND GLOBAL EXISTENCE OF WEAK SOLUTIONS

We start off here with a brief description of the wave-front tracking method to be employed throughout in Sections 4–7 and then establish the existence of entropy solutions when the perturbation of the incoming flow has small total variation at $x = 0$.

The main scheme in the method of wave-front tracking is to construct approximate solutions within a class of piecewise constant functions. At the beginning, we approximate the initial data by a piecewise constant function. Then we solve the resulting Riemann problems exactly with the exception of the rarefaction waves, which are replaced by rarefaction fans with many small wave-fronts of equal strengths. The outgoing fronts are continued up to the first time when two waves collide and a new Riemann problem is solved. In this process, one has to modify the algorithm and introduce a simplified Riemann solver in order to keep the number of wave-fronts finite for all $x \geq 0$ in the flow direction. We refer the reader to Bressan [3, 5] and Baiti-Jenssen [1] for related references.

3.1. The Riemann Solvers. As seen in Section 2, the solution to the Riemann problem $\{U_b, U_a\}$ is a self-similar solution given by at most five states separated by shocks, vortex sheets, entropy waves, or rarefaction waves. To connect the state U_a to U_b , there exist C^2 -curves $\eta \rightarrow \varphi(\eta)(U)$ with arc length parametrization such that

$$U_b = \varphi(\eta)(U_a) := \Upsilon_4(\eta_4) \circ \cdots \circ \Upsilon_1(\eta_1)(U_a)$$

for some $\eta = (\eta_1, \dots, \eta_4)$, and $U_j = \Upsilon_j(\eta_j) \circ \cdots \circ \Upsilon_1(\eta_1)(U_a)$, $j = 1 \dots 3$.

Next, we discuss the construction of front tracking approximations for our initial-boundary value problem. Let ϑ denote the initial approximation parameter. For given initial data \bar{U} and with $\vartheta > 0$, consider \bar{U}^ϑ a sequence of piecewise constant functions approximating \bar{U} in the L^1 -norm, and the wall boundary is also approximated as described in Section 2. Set Z_ϑ to be the total number of jumps in the initial data \bar{U}^ϑ and the tangential angle function of the wall boundary. Let $\delta_\vartheta > 0$ be a parameter so that a rarefaction wave is replaced by a step function whose ‘‘steps’’ are no further apart than δ_ϑ . The discontinuity between two steps is set to propagate with a speed equal to the Rankine-Hugoniot speed of the jump connecting the states corresponding to the two steps. At any time, the simplified Riemann solver (defined below) is employed, the constant $\hat{\lambda}$ denotes the speed of the generated non-physical wave, which is strictly greater than all the wave speeds of system (2.1). Note that the strength of the non-physical wave is the error generated when the simplified Riemann solver is applied.

Accurate Riemann solver. The accurate Riemann solver (**ARS**) is the exact solution to the Riemann problem, with the condition that every rarefaction wave $\{w, R_d(w)(\alpha)\}$, $d = 1, 4$, is divided into equal parts and replaced by a piecewise constant rarefaction fan of several new wave-fronts of equal strength.

Simplified Riemann solver. When only weak waves are involved, the simplified Riemann solver (**SRS**) here is the same as the one described in [1, 5]. That is, all new waves are put together in a single *non-physical front*, travelling faster than all characteristic speeds. In the case of a weak wave interacting with the strong vortex sheet/entropy wave, the purpose of (**SRS**) is to ignore the strength of the weak wave, while preserving the strength of the strong vortex sheet/entropy wave, and to place the error in the non-physical wave in the following manner:

Case 1 : A weak wave $\{U_-, U_1\}$ collides with the strong vortex sheet/entropy wave $\{U_1, U_+\}$ from below. The Riemann problem $\{U_-, U_+\}$ is solved as follows:

$$\begin{cases} U_- & \text{for } \frac{y}{x} < \chi(U_1, U_+), \\ U_2 & \text{for } \chi(U_1, U_+) < \frac{y}{x} < \hat{\lambda}, \\ U_+ & \text{for } \frac{y}{x} > \hat{\lambda}, \end{cases}$$

with $\chi(U_1, U_+)$ as the speed of the strong vortex sheet/entropy wave, and the state U_2 is solved in a way that $\{U_-, U_2\}$ is the strong vortex sheet/entropy wave starting from U_- and $\chi(U_1, U_+) = \chi(U_-, U_2)$. Hence, we find that (**SRS**) keeps the same strength of the strong vortex sheet/entropy wave, and the error appears in the non-physical fronts.

Case 2: A weak wave $\{U_2, U_+\}$ collides with the strong vortex sheet/entropy wave $\{U_-, U_2\}$ from above. The Riemann problem $\{U_-, U_+\}$ is solved as follows:

$$\begin{cases} U_- & \text{for } \frac{y}{x} < \chi(U_-, U_2), \\ U_2 & \text{for } \chi(U_-, U_2) < \frac{y}{x} < \hat{\lambda}, \\ U_+ & \text{for } \frac{y}{x} > \hat{\lambda}, \end{cases}$$

with $\chi(U_-, U_2)$ denoting the speed of the strong vortex sheet/entropy wave.

3.2. Construction of Wave Front Tracking Approximations

Given ϑ , the corresponding front tracking approximate solution $U^\vartheta(x, y)$ is built up as follows. At $x = 0$, all the Riemann problems in \bar{U}^ϑ are solved by using the accurate Riemann solver. Furthermore, one can change the speed of one of the incoming fronts so that, at any time $x > 0$, there is at most one collision involving only two incoming fronts. Of course, this adjustment of speed can be chosen arbitrarily small. Let ω_ϑ be a fixed small parameter with $\omega_\vartheta \rightarrow 0$, as $\vartheta \rightarrow 0$, which will be determined later. For convenience, the index j in α_j will be dropped henceforward, and we will write α_j as α when there is no ambiguity involved; the same applies for β ; and we will moreover employ the same notation α as a wave and its strength as before.

Case 1: Two weak waves with strengths α and β interact at some $x > 0$. The Riemann problem produced by this collision is solved in the following way:

- If $|\alpha\beta| > \omega_\vartheta$ and the two waves are physical, then the accurate Riemann solver is employed.
- If $|\alpha\beta| < \omega_\vartheta$ and the two waves are physical, or there is a non-physical wave, then the simplified Riemann solver is employed.

Case 2: A weak wave α interacts with the strong vortex sheet/entropy wave and one weak wave at some $x > 0$. The Riemann problem produced by this collision is solved in the following way:

- If $|\alpha| > \omega_\vartheta$ and the weak wave is physical, then the accurate Riemann solver is applied.
- If $|\alpha| < \omega_\vartheta$ and the weak wave is physical, or this wave is non-physical, then the simplified Riemann solver is applied.

Case 3: The flow perturbation due to the Lipschitz wall boundary.

- When the change of the angle of the boundary is larger than ω_ϑ and the weak wave is physical, then the accurate Riemann solver is employed to solve the lateral Riemann problem.
- If the change of the angle of the boundary is less than ω_ϑ , then this perturbation is ignored.

Case 4: The physical wave collides with the boundary. The accurate Riemann solver is employed to solve the lateral Riemann problem.

Case 5: The non-physical wave collides with the boundary. We can allow these waves to cross the boundary.

3.3. Glimm's Functional and Wave Interaction Potential

The goal in this subsection is to construct the suitable Glimm-type functional and the associated wave interaction potential \mathcal{Q} for our initial-boundary value problem. This involves a careful incorporation of the additional nonlinear waves generated from the wall boundary vertices.

Definition 3.1 (*Approaching waves*). (i) Two weak fronts α and β , located at points $y_\alpha < y_\beta$ and of the characteristic families $j_\alpha, j_\beta \in \{1, \dots, 4\}$, respectively, are said to be approaching each other if the following two conditions are concurrently satisfied:

- y_α and y_β are both in one of the two intervals into which \mathbb{R} is partitioned by the location of the strong vortex sheet/entropy wave. That is, both waves are either in Ω_- or Ω_+ ;
- Either $j_\alpha > j_\beta$ or else $j_\alpha = j_\beta$ and at least one of them is a genuinely nonlinear shock.

In this case, we write $(\alpha, \beta) \in \mathcal{A}$.

(ii) We say that a weak wave α of the characteristic family j_α is approaching the strong vortex sheet/entropy wave if either $\alpha \in \Omega_-$ and $j_\alpha = 4$, or $\alpha \in \Omega_+$ and $j_\alpha = 1$. We then write $\alpha \in \mathcal{A}_{v/e}$.

(iii) We say that a weak wave α of the characteristic family j_α is approaching the boundary if $\alpha \in \Omega_-$ and $j_\alpha = 1$. We then write $\alpha \in \mathcal{A}_b$.

Define the total (weighted) strength of weak waves in $U^\vartheta(x, \cdot)$ as

$$\mathcal{V}(x) = \sum_{\alpha} |b_{\alpha}|.$$

Here, for a weak wave α of the j -family, its weighted strength is defined as

$$b_{\alpha} = \begin{cases} k_+ \alpha & \text{if } \alpha \in \Omega_+ \text{ and } j_{\alpha} = 1, \\ \alpha & \text{if } \alpha \in \Omega_-, \end{cases} \quad (3.1)$$

where $k_+ = \frac{2K_{21}}{K^*}$ and the coefficient K_{21} as given in Lemma 2.6.

Next, the wave interaction potential $\mathcal{Q}(x)$ is defined as

$$\begin{aligned} \mathcal{Q}(x) &= C^* \sum_{(\alpha, \beta) \in \mathcal{A}} |b_{\alpha} b_{\beta}| + K^* \sum_{\alpha \in \mathcal{A}_{v/e}} |b_{\alpha}| + \sum_{\beta \in \mathcal{A}_b} |b_{\beta}| + \widetilde{K}_{b0} \sum_{a_l > x} |\omega_l| \\ &= \mathcal{Q}_{\mathcal{A}} + \mathcal{Q}_{v/e} + \mathcal{Q}_b + \mathcal{Q}_{\Theta}. \end{aligned} \quad (3.2)$$

Here the constants $K^* \in (K_{11}, 1)$ and $\widetilde{K}_{b0} > K_{b0}$, while C^* is a constant to be specified later. To control the total variation of the new waves produced by the boundary vertices, \mathcal{Q}_{Θ} in our wave interaction potential $\mathcal{Q}(x)$ is an added term, compared to that for the Cauchy problem.

The Glimm-type functional \mathcal{G} is defined as follows

$$\mathcal{G}(x) = \mathcal{V}(x) + \kappa \mathcal{Q}(x) + |U^\diamond(x) - U_0^+| + |U_\diamond(x) - U_0^-|, \quad (3.3)$$

where the states $U_\diamond(x)$ and $U^\diamond(x)$ are the below state and the above state of the strong vortex sheet/entropy wave respectively at “time” x , U_0^- and U_0^+ are the below and above state of the strong vortex sheet/entropy wave respectively at $x = 0$, and κ is a large positive constant to be determined later.

We remark that \mathcal{V} , \mathcal{Q} , and \mathcal{G} remain unchanged between any pair of subsequent interaction times. However, we will demonstrate that, across an interaction “time” x , both \mathcal{Q} and \mathcal{G} decrease.

Proposition 3.1. *Assume that $\text{TV}(\widetilde{U}_0(\cdot)) + \text{TV}(g'(\cdot))$ is sufficiently small. Then $V(x)$ will remain sufficiently small for all $x > 0$. Moreover, the quantity $\text{TV}(U^\vartheta(x, \cdot))$ has a uniform bound for any $\vartheta > 0$.*

Proof. With the Glimm-type functional \mathcal{G} , consider

$$\Delta \mathcal{G}(x) = \mathcal{G}(x^+) - \mathcal{G}(x^-),$$

where x^- and x^+ denote the “times” before and after the interaction “time” $x > 0$, respectively.

Case 1: Two weak waves α and β collide. Then the states $U^\diamond(x)$ and $U_\diamond(x)$ do not alter across this interaction “time” $x > 0$. Hence, we have

$$\begin{aligned} \Delta \mathcal{G}(x) &= \mathcal{V}(x^+) - \mathcal{V}(x^-) + \kappa (\mathcal{Q}(x^+) - \mathcal{Q}(x^-)) \\ &\leq \mathcal{B}_1 |b_\alpha b_\beta| + \kappa (-C^* |b_\alpha b_\beta| + C^* |b_\alpha b_\beta| V(x^-) + \mathcal{B}_0 |b_\alpha b_\beta|), \end{aligned}$$

where \mathcal{B}_0 and \mathcal{B}_1 are constants independent of ϑ .

Case 2: A weak wave α of the 1-family interacts with the boundary.

$$\Delta \mathcal{G}(x) = K_{b1} \alpha - \alpha + \kappa (C^* K_{b1} V(x^-) \alpha + K^* K_{b1} \alpha - \alpha),$$

where $K^* K_{b1} < 1$.

Case 3: A new 4-wave α produced by the Lipschitz wall boundary.

$$\Delta \mathcal{G}(x) = K_{b0} \theta_l + \kappa (C^* K_{b0} \theta_l V(x^-) + K^* K_{b0} \theta_l - \widetilde{K}_{b0} \theta_l),$$

where $K_{b0} < \widetilde{K}_{b0}$ is large.

In the following two cases, the states $U_\diamond(x)$ and $U^\diamond(x)$ change across this interaction “time” $x > 0$.

Case 4: A weak wave α of the 4-family collides with the strong vortex sheet/entropy wave from below.

$$\begin{aligned} \Delta \mathcal{G}(x) &= \mathcal{V}(x^+) - \mathcal{V}(x^-) + |U^\diamond(x^+) - U^\diamond(x^-)| \\ &\quad + |U_\diamond(x^+) - U_\diamond(x^-)| + \kappa (\mathcal{Q}(x^+) - \mathcal{Q}(x^-)) \\ &= \sum_{j=1}^4 K_{1j} \alpha - \alpha + \kappa (C^* (K_{11} V(x^-) \alpha + K_{14} V(x^-) \alpha) - K^* \alpha + K_{11} \alpha). \end{aligned}$$

Case 5: A weak wave α of the 1-family collides with the strong vortex sheet/entropy wave from above.

$$\Delta \mathcal{G}(x) = \sum_{j=1}^4 K_{2j} \alpha - b_\alpha + \kappa (C^* (K_{21} V(x^-) \alpha + K_{24} V(x^-) \alpha) - K^* b_\alpha + K_{21} \alpha).$$

In the cases above, $K_{11} < K^* < 1$, $b_\alpha > 2K_{21} |\alpha|$ in connection with the weight k_+ , and the constant $C^* > \mathcal{B}_0 > 0$ is large.

Next, we establish that the *total (weighted) strength of waves* in $U^\vartheta(x, \cdot)$ remain sufficiently small for all $x > 0$ if it is sufficiently small at $x = 0$. More precisely,

$$\mathcal{V}(x) \ll 1 \quad \text{for all } x > 0.$$

This can be proved as follows:

(i) “Time” $x_1 > 0$ is the first interaction. Given that $\mathcal{V}(x_1^-) = \mathcal{V}(0) \leq \text{TV}(\widetilde{U}_0(\cdot)) \ll 1$ and $\sum_{l=0}^{\infty} \theta_l \leq \text{TV}(g'(\cdot)) \ll 1$ in Cases 1–5 above, we conclude that, for κ sufficiently large and ω_ϑ small enough,

$$\Delta \mathcal{G}(x_1) \leq 0, \quad \text{i.e.,} \quad \mathcal{G}(x_1^+) \leq \mathcal{G}(x_1^-) = \mathcal{G}(0).$$

Therefore,

$$\begin{aligned} \mathcal{V}(x_1^+) &\leq \mathcal{G}(x_1^+) \leq \mathcal{G}(0) \leq \mathcal{V}(0) + \kappa \mathcal{Q}(0) \\ &= \mathcal{V}(0) + \kappa \left(C^* \mathcal{V}^2(0) + \mathcal{V}(0) + \widetilde{K}_{b0} \sum_{l=0}^{\infty} \theta_l \right) \\ &\leq C \left(\mathcal{V}(0) + \sum_{l=0}^{\infty} \theta_l \right) \ll 1. \end{aligned}$$

(ii) $\mathcal{V}(x_m^-) \ll 1$ and $\mathcal{G}(x_m^+) \leq \mathcal{G}(x_m^-)$ for any $m < n$. Then, for the next interaction “time” x_n , similar to Case 1, we also conclude

$$\Delta \mathcal{G}(x_n) \leq 0, \quad \text{i.e.,} \quad \mathcal{G}(x_n^+) \leq \mathcal{G}(x_n^-) = \mathcal{G}(x_{n-1}^+).$$

Therefore, all together, we obtain

$$\begin{aligned} \mathcal{V}(x_n^+) + |U^\diamond(x_n^+) - U_0^+| + |U_\circ(x_n^+) - U_0^-| \\ &\leq \mathcal{G}(x_n^+) \leq \mathcal{G}(x_n^-) = \mathcal{G}(x_{n-1}^+) \leq \dots \leq \mathcal{G}(0) \\ &= \mathcal{V}(0) + \kappa \mathcal{Q}(0) \\ &= \mathcal{V}(0) + \kappa \left(C^* \mathcal{V}^2(0) + \mathcal{V}(0) + \widetilde{K}_{b0} \sum_{l=0}^{\infty} \theta_l \right) \\ &\leq C \left(\mathcal{V}(0) + \sum_{l=0}^{\infty} \theta_l \right) \ll 1. \end{aligned}$$

This implies that $\mathcal{V}(x) \ll 1$ for all $x > 0$, since C is independent of x .

Furthermore, the total variation of $U^\vartheta(x, \cdot)$ is uniformly bounded. More precisely, we conclude that

$$\text{TV}\{U^\vartheta(x, \cdot)\} \approx V(x) + |U^\diamond(x) - U_0^+| + |U_\circ(x) - U_0^-| + |\sigma_{20}| + |\sigma_{30}| = \mathcal{O}(1). \quad (3.4)$$

This completes the proof.

In order to have a front tracking approximate solution $U^\vartheta(x, \cdot)$ defined for any time $x > 0$, along with a uniform bound on the total variation, we also need to have that the number of wave-fronts in $U^\vartheta(x, \cdot)$ is finite. This is given by the subsequent lemma.

Lemma 3.2. *For any fixed $\vartheta > 0$ small enough, the number of wave-fronts in $U^\vartheta(x, y)$ is finite and the approximate solutions $U^\vartheta(x, y)$ are defined for all $x > 0$. Moreover, for any $x > 0$, the total strength of the all non-physical waves is of order $\mathcal{O}(1)$ ($\delta_\vartheta + \omega_\vartheta$).*

Proof. We first note the total interaction potential $\mathcal{Q}(x)$ remains unchanged when there is no interaction and decreases across an interaction “time” $x > 0$ as discussed in Cases 1–5 in Proposition 3.1. Furthermore, from Cases 1–5 and the subsequent analysis above, we have concluded that $\mathcal{V}(x) \ll 1$. Hence, one can fix some number $\nu \in (0, 1)$ such that

$$\begin{aligned} \Delta \mathcal{Q}(x) &= \mathcal{Q}(x^+) - \mathcal{Q}(x^-) \\ &\leq \begin{cases} -\nu |b_\alpha b_\beta| & \text{if both waves } \alpha \text{ and } \beta \text{ are weak,} \\ -\nu |b_\alpha| & \text{if the weak wave } \alpha \text{ hits the strong vortex sheet/entropy wave,} \\ -\nu |\theta_l| & \text{if the angle of the boundary changes.} \end{cases} \end{aligned} \quad (3.5)$$

Now, following an argument similar to the one given in [1], we reach the following conclusions. Note that initially $\mathcal{Q}(0)$ is bounded and \mathcal{Q} decreases thereafter for each case. Moreover, in the case where the interaction potential between the incoming waves or the change of the angle of the

boundary is larger than ω_ϑ , Q decreases by at least $\nu\omega_\vartheta$ in these interactions, as implied by the bounds given in (3.5). Following the wave-front tracking method in our problem, new physical waves can be only produced by such interactions. Furthermore, when the weak wave α of 1-family collides with the wall boundary, we solve the lateral Riemann problem and have shown earlier that, after this interaction, there is only a reflected wave of 4-family with the reflection coefficient 1. Hence, before and after this interaction, the number of the waves keeps the same, and this implies that the number of the waves is finite. Finally, because non-physical waves are generated only when physical waves collide, we can also conclude that the number of non-physical wave fronts are finite; and, provided that two waves can only collide once, the number of interactions is also finite. Consequently, it follows that the approximate solutions $U^\vartheta(x, \cdot)$ are defined for all times $x > 0$. The similar argument allows us to conclude that the total strength of all non-physical wave fronts at any x is of order $\mathcal{O}(1)(\delta_\vartheta + \omega_\vartheta)$. This completes the proof Lemma 3.2.

Following the line of arguments given in [1, 3] for the wave-front tracking algorithm and Lemma 3.1 above, we finish this section with the following theorem for the global existence of entropy solutions to the initial-boundary value problem (1.1) and (1.7)–(1.8).

Theorem 3.1. *Suppose that $\text{TV}(\widetilde{U}_0(\cdot)) + \text{TV}(g'(\cdot))$ is small enough. Then, for the initial-boundary value problem (1.1) and (1.7)–(1.8), there exists a global weak solution in BV satisfying the steady Clausius entropy inequality (1.9).*

4. THE LYAPUNOV FUNCTIONAL FOR THE L^1 -DISTANCE BETWEEN TWO SOLUTIONS

To show that the front tracking approximations, constructed for the existence analysis in Section 3, converge to a unique limit, we estimate the distance between any two ϑ -approximate U and V of problem (1.1) and (1.7)–(1.8) of initial-boundary value type. To this end, we develop the Lyapunov functional $\Phi(U, V)$, equivalent to the L^1 -distance:

$$C^{-1} \|U(x, \cdot) - V(x, \cdot)\|_{L^1} \leq \Phi(U, V) \leq C \|U(x, \cdot) - V(x, \cdot)\|_{L^1},$$

and prove that the functional $\Phi(U, V)$ is *almost decreasing* along pairs of solutions,

$$\Phi(U(x_2, \cdot), V(x_2, \cdot)) - \Phi(U(x_1, \cdot), V(x_1, \cdot)) \leq C\vartheta(x_2 - x_1), \quad \text{for all } x_2 > x_1 > 0,$$

for some constant $C > 0$. Here U and V are two approximate solutions constructed via the wave-front tracking method, and the small approximation parameter ϑ is responsible for controlling the subsequent errors:

- Errors in the approximation of the initial data and the boundary.
- Errors in the speeds of shock, vortex sheet, entropy wave, and rarefaction fronts.
- The total strength of all non-physical fronts.
- The maximum strength of rarefaction fronts.

Along the line of arguments presented in [8, 21, 23], with “time” x fixed, at each y , one connects the state $U(y)$ with $V(y)$ in the state space by going along the Hugoniot curves S_1, C_2, C_3 , and S_4 . Depending on the location of the strong vortex sheet/entropy wave in $U(y)$ and $V(y)$, the distance between $U(y)$ and $V(y)$ is estimated along discontinuity waves in possibly different “directions”, determining the strength of the j -Hugoniot wave $h_j(y)$ in the following way:

- Suppose that $U(y)$ and $V(y)$ are both in Ω_- and Ω_+ . Then one begins at the state $U(y)$ and moves along the Hugoniot curves to reach the state $V(y)$.
- Suppose that $U(y)$ is in Ω_- and $V(y)$ is in Ω_+ . Then one begins at the state $U(y)$ and moves along the Hugoniot curves to reach the state $V(y)$.
- Suppose that $V(y)$ is in Ω_- and $U(y)$ is in Ω_+ . Then one begins at the state $V(y)$ and moves along the Hugoniot curves to reach the state $U(y)$.

Define the L^1 -weighted strengths of the waves in the solution of the Riemann problem $(U(y), V(y))$ or $(V(y), U(y))$ as follows:

$$q_j(y) = \begin{cases} w_j^b \cdot h_j(y) & \text{whenever } U(y) \text{ and } V(y) \text{ are both in } \Omega_-, \\ w_j^m \cdot h_j(y) & \text{whenever } U(y) \text{ and } V(y) \text{ are both in different domains,} \\ w_j^a \cdot h_j(y) & \text{whenever } U(y) \text{ and } V(y) \text{ are both in } \Omega_+, \end{cases} \quad (4.1)$$

with the constants w_j^b , w_j^m , and w_j^a above to be specified later on, based on the estimates of wave interactions and reflections in Lemmas 2.2–2.7.

We define the following Lyapunov functional,

$$\Phi(U, V) = \sum_{j=1}^4 \int_{g(x)}^{\infty} |q_j(y)| W_j(y) dy, \quad (4.2)$$

where the weights are given by

$$W_j(y) = 1 + \kappa_1 A_j(y) + \kappa_2 (\mathcal{Q}(U) + \mathcal{Q}(V)). \quad (4.3)$$

The constants κ_1 and κ_2 are to be determined later. Here \mathcal{Q} denotes the total wave interaction potential incorporating the boundary effect as defined in (3.2), and $A_j(y)$ denotes the total strength of waves in U and V , which approach the j -wave $q_j(y)$, defined in the following manner (for y where there is no jump in U or V):

$$A_j(y) = F_j(y) + G_j(y) + \begin{cases} H_j(y) & \text{if } j\text{-wave } q_j(y) \text{ is small and the } j\text{-field is genuinely nonlinear,} \\ 0 & \text{if } j = 2, 3 \text{ and } q_j(y) = B \text{ is large.} \end{cases} \quad (4.4)$$

Next, we define the following global weights G_j :

$G_j(y) =$	U, V are both in Ω_-	U, V are in distinct regions	U, V are both in Ω_+
$G_1(y)$	4B	2B	4B
$G_{2,3}(y)$	0	0	0
$G_4(y)$	4B	2B	2B

Under the assumption that $\text{TV}(\widetilde{U}_0(\cdot)) + \text{TV}(\widetilde{V}_0(\cdot)) + \text{TV}(g'(\cdot))$ is small enough with $U(x, \cdot), V(x, \cdot) \in \text{BV} \cap L^1$, one concludes

$$\mathcal{M}^{-1} \|U(x, \cdot) - V(x, \cdot)\|_{L^1} \leq \sum_{j=1}^4 \int_{g(x)}^{\infty} |q_j(y)| dy \leq \mathcal{M} \|U(x, \cdot) - V(x, \cdot)\|_{L^1},$$

$$1 \leq W_j(y) \leq \mathcal{M}, \quad j = 1, \dots, 4,$$

where the constant \mathcal{M} is independent of ϑ and “time” x . Here we define the strength of any large wave of the 2- or 3-characteristic family to equal to some fixed number B (bigger than all strengths of small waves), and the concepts “small” and “large” mean the waves that connect the states in the same or in the distinct domains Ω^- and Ω^+ , respectively.

The summands in (4.4) are defined as follows,

$$F_j(y) = \left(\sum_{\substack{\alpha \in \mathcal{J} \setminus \mathcal{SC} \\ y_\alpha < y, j < k_\alpha \leq 4}} + \sum_{\substack{\alpha \in \mathcal{J} \setminus \mathcal{SC} \\ y_\alpha > y, 1 \leq k_\alpha < j}} \right) |\alpha|,$$

$$H_j(y) = \begin{cases} \left(\sum_{\alpha \in \mathcal{J}(U) \setminus \mathcal{SC}, y_\alpha < y, k_\alpha = j} + \sum_{\alpha \in \mathcal{J}(V) \setminus \mathcal{SC}, y_\alpha > y, k_\alpha = j} \right) |\alpha| & \text{if } q_j(y) < 0, \\ \left(\sum_{\alpha \in \mathcal{J}(V) \setminus \mathcal{SC}, y_\alpha < y, k_\alpha = j} + \sum_{\alpha \in \mathcal{J}(U) \setminus \mathcal{SC}, y_\alpha > y, k_\alpha = j} \right) |\alpha| & \text{if } q_j(y) > 0, \end{cases}$$

where, at each x , α stands for the (non-weighted) strength of the wave $\alpha \in \mathcal{J}$, located at the point y_α and belonging to the characteristic family k_α ; $\mathcal{J} = \mathcal{J}(U) \cup \mathcal{J}(V)$, $\mathcal{SC} = \mathcal{SC}(U) \cup \mathcal{SC}(V)$ is the set of all waves (in U and V) and the set of all large (strong) characteristic discontinuities (in U and V) respectively.

Consequently, there holds

$$C^{-1}\|U(x, \cdot) - V(x, \cdot)\|_{L^1} \leq \Phi(U, V) \leq C\|U(x, \cdot) - V(x, \cdot)\|_{L^1}, \quad (4.5)$$

for any $x \geq 0$ with the constant $C > 0$ depending only on the quantities independent of x : the strength of the strong vortex sheet/entropy wave and $\text{TV}(\widetilde{U}_0(\cdot)) + \text{TV}(\widetilde{V}_0(\cdot)) + \text{TV}(g'(\cdot))$.

We now analyze the evolution of the Lyapunov functional Φ in the flow direction $x > 0$. For $j = 1, \dots, 4$, we call $\lambda_j(y)$ the speed of the j -wave $q_j(y)$ (along the Hugoniot curve in the phase space). Then, at a ‘‘time’’ $x > 0$ which is not the interaction time of the waves either in $U(x) = U(x, \cdot)$ or $V(x) = V(x, \cdot)$, an explicit computation gives

$$\begin{aligned} & \frac{d}{dx} \Phi(U(x), V(x)) \\ &= \sum_{\alpha \in \mathcal{J}} \sum_{j=1}^4 (|q_j(y_\alpha^-)|W_j(y_\alpha^-) - |q_j(y_\alpha^+)|W_j(y_\alpha^+)) \dot{y}_\alpha + \sum_{j=1}^4 |q_j(b)|W_j(b)\dot{y}_b \\ &= \sum_{\alpha \in \mathcal{J}} \sum_{j=1}^4 (|q_j(y_\alpha^-)|W_j(y_\alpha^-) (\dot{y}_\alpha - \lambda_j(y_\alpha^-)) - |q_j(y_\alpha^+)|W_j(y_\alpha^+) (\dot{y}_\alpha - \lambda_j(y_\alpha^+))) \\ & \quad + \sum_{j=1}^4 |q_j(b)|W_j(b) (\dot{y}_b + \lambda_j(b)), \end{aligned} \quad (4.6)$$

where \dot{y}_α denotes the speed of the Hugoniot wave $\alpha \in \mathcal{J}$, $b = g(x)^+$ stands for the points close to the boundary, and \dot{y}_b is the slope of the boundary.

We present the notation

$$E_{\alpha,j} = |q_j^+|W_j^+ (\lambda_j^+ - \dot{y}_\alpha) - |q_j^-|W_j^- (\lambda_j^- - \dot{y}_\alpha), \quad (4.7)$$

$$E_{b,j} = |q_j(b)|W_j(b) (\dot{y}_b + \lambda_j(b)), \quad (4.8)$$

where $q_j^\pm = q_j(y_\alpha^\pm)$, $W_j^\pm = W_j(y_\alpha^\pm)$, and $\lambda_j^\pm = \lambda_j(y_\alpha^\pm)$.

Then (4.6) can be written as

$$\frac{d}{dx} \Phi(U(x), V(x)) = \sum_{\alpha \in \mathcal{J}} \sum_{j=1}^4 E_{\alpha,j} + \sum_{j=1}^4 E_{b,j}. \quad (4.9)$$

Our central aim is to prove the bounds:

$$\sum_{j=1}^4 E_{\alpha,j} \leq \mathcal{O}(1)\vartheta|\alpha| \quad \text{when } \alpha \text{ is a weak wave in } \mathcal{J}, \quad (4.10)$$

$$\sum_{j=1}^4 E_{\alpha,j} \leq \mathcal{O}(1)|\alpha| \quad \text{when } \alpha \text{ is a non-physical wave in } \mathcal{J}, \quad (4.11)$$

$$\sum_{j=1}^4 E_{\alpha,j} \leq 0 \quad \text{when } \alpha \text{ is a strong vortex sheet/entropy wave in } \mathcal{J}, \quad (4.12)$$

$$\sum_{j=1}^4 E_{b,j} \leq 0 \quad \text{near the boundary}, \quad (4.13)$$

where the quantities denoted by the Landau symbol $\mathcal{O}(1)$ are independent of the constants κ_1 and κ_2 .

From (4.10)–(4.13) together with the uniform bound on the total strengths of waves (3.4), we obtain

$$\frac{d}{dx} \Phi(U(x), V(x)) \leq \mathcal{O}(1)\vartheta. \quad (4.14)$$

Integration of (4.14) over the interval $[0, x]$ yields

$$\Phi(U(x), V(x)) \leq \Phi(U(0), V(0)) + \mathcal{O}(1)\vartheta x. \quad (4.15)$$

We remark that, at each interaction “time” x when two fronts of U or two fronts of V interact, by the Glimm interaction estimates, all the weight functions $W_j(y)$ decrease, if the constant κ_2 in the Lyapunov functional is taken to be sufficiently large. Furthermore, due to the self-similar property of the Riemann solutions, Φ decreases at this “time”.

In the next section, we establish the bounds (4.10)–(4.13), particularly (4.12) and (4.13), when α is a strong vortex sheet/entropy wave in \mathcal{J} and near the Lipschitz wall boundary, respectively.

5. THE L^1 -STABILITY ESTIMATES

For the case of the non-physical waves in \mathcal{J} , as well as the case that the weak wave $\alpha \in \mathcal{J} := \mathcal{J}(U) \cup \mathcal{J}(V)$, which appears when U and V are both in Ω_- or Ω_+ , estimates (4.10) and (4.11) are shown similarly based on the arguments in Bressan-Liu-Yang [8], provided that $\frac{2|B|}{|\sigma_{20}| + |\sigma_{30}|}$ is sufficiently small and κ_1 is sufficiently large. In what follows, we focus only on the other two cases, namely (4.12) and (4.13).

Case 1: *The first strong vortex sheet/entropy wave α in U or V is crossed.* Then, by Lemma 2.4, we have the estimates:

$$h_1^+ = h_1^- + K_{11}h_4^-, \quad (5.1)$$

$$h_4^+ = K_{14}h_4^-. \quad (5.2)$$

Moreover, the essential estimate $|K_{11}| < 1$ given in Lemma 2.4 ensures the existence of desired weights w_1^b and w_4^b in the following way.

Lemma 5.1. *There exist w_1^b , w_4^b , and γ_b satisfying*

$$\frac{w_4^b}{w_1^b} < 1, \quad (5.3)$$

$$\frac{w_1^b}{w_4^b} K_{11} \left| \frac{\lambda_1^- - \lambda_{2,3}}{\lambda_4^- - \lambda_{2,3}} \right| < \gamma_b < 1. \quad (5.4)$$

With Lemma 5.1, we estimate E_j for $j = 1, \dots, 4$, starting with E_1 : By (5.1) and (5.4),

$$\begin{aligned} E_1 &= |q_1^-|(\lambda_1^- - \dot{y}_\alpha)(W_1^+ - W_1^-) + W_1^+ (|q_1^+|(\lambda_1^+ - \dot{y}_\alpha) - |q_1^-|(\lambda_1^- - \dot{y}_\alpha)) \\ &= 2B\kappa_1 w_1^b |h_1^-| |\lambda_1^- - \dot{y}_\alpha| + W_1^+ (|q_1^-| |\lambda_1^- - \dot{y}_\alpha| - |q_1^+| |\lambda_1^+ - \dot{y}_\alpha|) \\ &\leq 2B\kappa_1 w_1^b |h_1^-| |\lambda_1^- - \dot{y}_\alpha| + W_1^+ \left(w_1^b |h_1^+| |\lambda_1^- - \dot{y}_\alpha| + w_1^b K_{11} |h_4^-| |\lambda_1^- - \dot{y}_\alpha| - w_1^m |h_1^+| |\lambda_1^+ - \dot{y}_\alpha| \right) \\ &\leq 2B\kappa_1 w_1^b |h_1^-| |\lambda_1^- - \dot{y}_\alpha| + 2B\kappa_1 \left(w_1^b |h_1^+| |\lambda_1^- - \dot{y}_\alpha| + \gamma_b w_4^b |h_4^-| (\lambda_4^- - \dot{y}_\alpha) - w_1^m |h_1^+| |\lambda_1^+ - \dot{y}_\alpha| \right) \\ &\quad + (\kappa_1 A_{W_1^+} + M) |q_1^-| |\lambda_1^- - \dot{y}_\alpha| - (\kappa_1 A_{W_1^+} + M) |q_1^+| |\lambda_1^+ - \dot{y}_\alpha|, \end{aligned}$$

where $W_1^+ = W_1(y_\alpha^+) = 2B\kappa_1 + \kappa_1 A_{W_1^+} + M$, and $M = 1 + \kappa_2(\mathcal{Q}(U) + \mathcal{Q}(V))$ is a positive constant. The term $A_{W_1^+} = F_1(y_\alpha^+) + H_1(y_\alpha^+)$ here is the total strength of all the weak waves in U and V which approach the 1-wave $q_1^+ = q_1(y_\alpha^+)$, and the term $2B\kappa_1$ is from the weight $G_1(y_\alpha^+)$.

For $j = 2, 3$, since $W_j^+ = W_j^-$, (4.6) reduces to

$$E_j = W_j^- (|q_j^+|(\lambda_j^+ - \dot{y}_\alpha) - |q_j^-|(\lambda_j^- - \dot{y}_\alpha)) \leq \mathcal{O}(1)B \left(\vartheta + \sum_{i \neq \{2,3\}} |q_i^-| + |q_k^-| \right),$$

where $k \neq \{j, 1, 4\}$.

For $j = 4$,

$$\begin{aligned} E_4 &= |q_4^-|(\lambda_4^- - \dot{y}_\alpha)(W_4^+ - W_4^-) + W_4^+ (|q_4^+|(\lambda_4^+ - \dot{y}_\alpha) - |q_4^-|(\lambda_4^- - \dot{y}_\alpha)) \\ &= -2B\kappa_1|q_4^-|(\lambda_4^- - \dot{y}_\alpha) + (2B\kappa_1 + \kappa_1 A_{W_4^+} + M)|q_4^+|(\lambda_4^+ - \dot{y}_\alpha) \\ &\quad - (2B\kappa_1 + \kappa_1 A_{W_4^+} + M)|q_4^-|(\lambda_4^- - \dot{y}_\alpha), \end{aligned}$$

where $W_4^+ = W_4(y_\alpha^+) = 2B\kappa_1 + \kappa_1 A_{W_4^+} + M$, and $M = 1 + \kappa_2(\mathcal{Q}(U) + \mathcal{Q}(V))$ is a positive constant. The term $A_{W_4^+} = F_4(y_\alpha^+) + H_4(y_\alpha^+)$ is the total strength of all the weak waves in U and V which approach the 4-wave $q_4^+ = q_4(y_\alpha^+)$, and the term $2B\kappa_1$ is from the weight $G_4(y_\alpha^+)$.

For the weighted L^1 -strength $q_j(y)$ in (4.1), we choose w_1^b small enough relatively to w_1^m and w_4^b large enough relatively to w_4^m , choose κ_1 large enough and the total variation of U and V so small, and use (5.1)–(5.2) to obtain

$$\begin{aligned} \sum_{j=1}^4 E_j &\leq 2B\kappa_1 \left(w_1^b |h_1^+| |\lambda_1^- - \dot{y}_\alpha| + \gamma_b w_4^b |h_4^-| (\lambda_4^- - \dot{y}_\alpha) - w_1^m |h_1^+| |\lambda_1^+ - \dot{y}_\alpha| \right) \\ &\quad + (\kappa_1 A_{W_1^+} + M) |q_1^-| |\lambda_1^- - \dot{y}_\alpha| - (\kappa_1 A_{W_1^+} + M) |q_1^+| |\lambda_1^+ - \dot{y}_\alpha| \\ &\quad + 2B\kappa_1 w_1^b |h_1^-| |\lambda_1^- - \dot{y}_\alpha| - 2B\kappa_1 |q_4^-| (\lambda_4^- - \dot{y}_\alpha) \\ &\quad + (2B\kappa_1 + \kappa_1 A_{W_4^+} + M) w_4^m |K_{14} p_4^-| (\lambda_4^+ - \dot{y}_\alpha) \\ &\quad - (2B\kappa_1 + \kappa_1 A_{W_4^+} + M) |q_4^-| (\lambda_4^- - \dot{y}_\alpha) \\ &\quad + \mathcal{O}(1)B \left(2\vartheta + 2 \sum_{i \neq \{2,3\}} |q_i^-| + (|q_2^-| + |q_3^-|) \right) \\ &= -(1 - \gamma_b) 2B\kappa_1 w_4^b |h_4^-| (\lambda_4^- - \dot{y}_\alpha) \\ &\quad + (\kappa_1 A_{W_4^+} + M) (w_4^m |K_{14} h_4^-| (\lambda_4^+ - \dot{y}_\alpha) - w_4^b |h_4^-| (\lambda_4^- - \dot{y}_\alpha)) \\ &\quad + 2B\kappa_1 w_1^b (|h_1^+| + |h_1^-|) |\lambda_1^- - \dot{y}_\alpha| - 2B\kappa_1 w_1^m |h_1^+| |\lambda_1^+ - \dot{y}_\alpha| \\ &\quad + 2B\kappa_1 w_4^m |K_{14} h_4^-| (\lambda_4^+ - \dot{y}_\alpha) - 2B\kappa_1 w_4^b |h_4^-| (\lambda_4^- - \dot{y}_\alpha) \\ &\quad + (\kappa_1 A_{W_1^+} + M) w_1^b |h_1^-| |\lambda_1^- - \dot{y}_\alpha| - (\kappa_1 A_{W_1^+} + M) w_1^m |h_1^+| |\lambda_1^+ - \dot{y}_\alpha| \\ &\quad + \mathcal{O}(1)B \left(2\vartheta + 2 \sum_{i \neq \{2,3\}} |q_i^-| + (|q_2^-| + |q_3^-|) \right) \\ &\leq 0. \end{aligned}$$

Case 2: *The weak wave α between the two strong vortex sheets/entropy waves in U and V is crossed.* For $j = 1$, we have

$$\begin{aligned} E_1 &= |q_1^\pm| (W_1^+ - W_1^-) (\lambda_1^\pm - \dot{y}_\alpha) + W_1^\mp (|q_1^+| (\lambda_1^+ - \dot{y}_\alpha) - |q_1^-| (\lambda_1^- - \dot{y}_\alpha)) \\ &\leq \kappa_1 |q_1^\pm| |\alpha| |\lambda_1^\pm - \dot{y}_\alpha| + 2B\kappa_1 ((|q_1^+| - |q_1^-|) (\lambda_1^+ - \dot{y}_\alpha) + |q_1^-| (\lambda_1^+ - \lambda_1^-)) \\ &\leq \kappa_1 |q_1^\pm| |\alpha| |\lambda_1^\pm - \dot{y}_\alpha| + 2B\kappa_1 ((|q_1^+| - |q_1^-|) (\lambda_1^+ - \dot{y}_\alpha) + \mathcal{O}(1) |q_1^-| |\alpha|). \end{aligned}$$

For the cases when $j = 2, 3$, we have

$$\begin{aligned} E_j &= B \left((W_j^+ - W_j^-) (\lambda_j^\pm - \dot{y}_\alpha) + W_j^\mp (\lambda_j^\pm - \lambda_j^\mp) \right) \\ &\leq B \left(-\kappa_1 |\alpha| |\lambda_j^\pm - \dot{y}_\alpha| + \mathcal{O}(1) |\alpha| \right). \end{aligned}$$

For $j = 4$, we have

$$\begin{aligned} E_4 &= |q_4^\pm| (W_4^+ - W_4^-) (\lambda_4^\pm - \dot{y}_\alpha) + W_4^\mp (|q_4^+| (\lambda_4^+ - \dot{y}_\alpha) - |q_4^-| (\lambda_4^- - \dot{y}_\alpha)) \\ &\leq \kappa_1 |q_4^\pm| |\alpha| |\lambda_4^\pm - \dot{y}_\alpha| + 2B\kappa_1 ((|q_4^+| - |q_4^-|) (\lambda_4^+ - \dot{y}_\alpha) + |q_4^-| (\lambda_4^+ - \lambda_4^-)) \\ &\leq \kappa_1 |q_4^\pm| |\alpha| |\lambda_4^\pm - \dot{y}_\alpha| + 2B\kappa_1 ((|q_4^+| - |q_4^-|) (\lambda_4^+ - \dot{y}_\alpha) + \mathcal{O}(1) |q_4^-| |\alpha|). \end{aligned}$$

Then we have

$$\sum_{j=1}^4 E_j \leq \kappa_1 \mathcal{O}(1) \left(-|\alpha| + |\alpha| \sum_{k \neq \{2,3\}} |q_k^+| + |q_k^-| + \sum_{k \neq \{2,3\}} |q_k^+| - |q_k^-| \right) + \mathcal{O}(1)|\alpha|.$$

Since $||q_k^+| - |q_k^-|| \leq |q_k^+ - q_k^-| \leq \mathcal{O}(1)|\alpha|$ when $k \neq \{2, 3\}$, we obtain

$$\sum_{j=1}^4 E_j \leq 0$$

if all the weights w_j^m are small enough and κ_1 is sufficiently large.

Notice that the choice of the upper or lower superscripts depends on the family number k_α .

Case 3: *The second strong vortex sheet/entropy wave α in U or V is crossed.* For this case, by Lemma 2.6, we have

$$h_1^- = K_{21}h_1^+, \quad (5.5)$$

$$h_4^- = h_4^+ + K_{24}h_1^+. \quad (5.6)$$

Moreover, the essential estimate $|K_{24}| < 1$ in Lemma 2.6 ensures the existence of desired weights w_1^a and w_4^a in the following manner.

Lemma 5.2. *There exist w_1^a , w_4^a , and γ_a satisfying*

$$\frac{w_4^a}{w_1^a} \left| \frac{\lambda_4^+ - \lambda_{2,3}}{\lambda_1^+ - \lambda_{2,3}} \right| K_{24} < \gamma_a < 1. \quad (5.7)$$

With Lemma 5.2, we estimate E_j for $j = 1, \dots, 4$ as follows: By (5.5),

$$\begin{aligned} E_1 &= |q_1^-|(\lambda_1^- - \dot{y}_\alpha)(W_1^+ - W_1^-) + W_1^+ (|q_1^+|(\lambda_1^+ - \dot{y}_\alpha) - |q_1^-|(\lambda_1^- - \dot{y}_\alpha)) \\ &= -2B\kappa_1|q_1^-||\lambda_1^- - \dot{y}_\alpha| + (4B\kappa_1 + \kappa_1 A_{W_1^+} + M)|q_1^+|(\lambda_1^+ - \dot{y}_\alpha) \\ &\quad + w_1^m |K_{21}h_1^+|(4B\kappa_1 + A_{W_1^+} + M)|\lambda_1^- - \dot{y}_\alpha|, \\ &= -2B\kappa_1|q_1^-||\lambda_1^- - \dot{y}_\alpha| + w_1^m |K_{21}h_1^+|(4B\kappa_1 + \kappa_1 A_{W_1^+} + M)|\lambda_1^- - \dot{y}_\alpha| \\ &\quad - w_1^a |h_1^+|(2B\kappa_1 + \kappa_1 A_{W_1^+} + M)|\lambda_1^+ - \dot{y}_\alpha| - 2B\kappa_1 w_1^a |h_1^+||\lambda_1^+ - \dot{y}_\alpha|, \end{aligned}$$

where $W_1^+ = W_1(y_\alpha^+) = 4B\kappa_1 + \kappa_1 A_{W_1^+} + M$, and $M = 1 + \kappa_2(\mathcal{Q}(U) + \mathcal{Q}(V))$ is a positive constant. The term $A_{W_1^+} = F_1(y_\alpha^+) + H_1(y_\alpha^+)$ here is the total strength of all the weak waves in U and V which approach the 1-wave $q_1^+ = q_1(y_\alpha^+)$, and the term $4B\kappa_1$ is from the weight $G_1(y_\alpha^+)$.

For $j = 2, 3$, since $W_j^+ = W_j^-$, (4.6) reduces to

$$\begin{aligned} E_j &= W_j^+ (|q_j^+|(\lambda_j^+ - \dot{y}_\alpha) - |q_j^-|(\lambda_j^- - \dot{y}_\alpha)) \\ &\leq \mathcal{O}(1)B \left(\vartheta + \sum_{i \neq \{2,3\}} |q_i^+| + |q_k^+| \right), \end{aligned}$$

where $k \neq \{j, 1, 4\}$.

By (5.6) and (5.7),

$$\begin{aligned} E_4 &= |q_4^-|(\lambda_4^- - \dot{y}_\alpha)(W_4^+ - W_4^-) + W_4^+ (|q_4^+|(\lambda_4^+ - \dot{y}_\alpha) - |q_4^-|(\lambda_4^- - \dot{y}_\alpha)) \\ &= W_4^+ (|q_4^+|(\lambda_4^+ - \dot{y}_\alpha) - |q_4^-|(\lambda_4^- - \dot{y}_\alpha)) \\ &\leq W_4^+ (w_4^a |h_4^-|(\lambda_4^+ - \dot{y}_\alpha) + w_4^a K_{24} |h_1^+|(\lambda_4^+ - \dot{y}_\alpha) - w_4^m |h_4^-|(\lambda_4^- - \dot{y}_\alpha)) \\ &\leq 2B\kappa_1 (w_4^a |h_4^-|(\lambda_4^+ - \dot{y}_\alpha) + \gamma_a w_1^a |h_1^+||\lambda_1^+ - \dot{y}_\alpha| - w_4^m |h_4^-|(\lambda_4^- - \dot{y}_\alpha)) \\ &\quad + (\kappa_1 A_{W_4^+} + M)|q_4^+|(\lambda_4^+ - \dot{y}_\alpha) - (\kappa_1 A_{W_4^+} + M)|q_4^-|(\lambda_4^- - \dot{y}_\alpha), \end{aligned}$$

where $W_4^+ = W_4(y_\alpha^+) = 2\kappa_1 B + \kappa_1 A_{W_4^+} + M$, and $M = 1 + \kappa_2(\mathcal{Q}(U) + \mathcal{Q}(V))$ is a positive constant. The term $A_{W_4^+} = F_4(y_\alpha^+) + H_4(y_\alpha^+)$ here is the total strength of all the weak waves in U and V which approach the 4-wave $q_4^+ = q_4(y_\alpha^+)$, and the term $2B\kappa_1$ is from the weight $G_4(y_\alpha^+)$.

For the weighted L^1 -strength $q_j(y)$ in (4.1), when w_4^a is small enough relatively to w_4^m and w_1^a is large enough relatively to w_1^m , κ_1 is large enough, applying (5.5) and (5.6), the total variation of u and v is so small that

$$\begin{aligned}
 \sum_{j=1}^4 E_j &\leq 2B\kappa_1 (w_4^a |h_4^-| (\lambda_4^+ - \dot{y}_\alpha) + \gamma_a w_1^a |h_1^+| |\lambda_1^+ - \dot{y}_\alpha| - w_4^m |h_4^-| (\lambda_4^- - \dot{y}_\alpha)) \\
 &\quad + (\kappa_1 A_{W_4^+} + M) |q_4^+| (\lambda_4^+ - \dot{y}_\alpha) - (\kappa_1 A_{W_4^+} + M) |q_4^-| (\lambda_4^- - \dot{y}_\alpha) \\
 &\quad - 2B\kappa_1 |q_1^-| |\lambda_1^- - \dot{y}_\alpha| - 2B\kappa_1 |q_1^+| |\lambda_1^+ - \dot{y}_\alpha| \\
 &\quad + (4B\kappa_1 + \kappa_1 A_{W_1^+} + M) w_1^m |K_{21} h_1^+| |\lambda_1^- - \dot{y}_\alpha| \\
 &\quad - (2B\kappa_1 + \kappa_1 A_{W_1^+} + M) w_1^a |h_1^+| |\lambda_1^+ - \dot{y}_\alpha| \\
 &\quad + \mathcal{O}(1)B \left(2\vartheta + 2 \sum_{i \neq \{2,3\}} |q_i^+| + (|q_2^+| + |q_3^+|) \right) \\
 &= -(1 - \gamma_a) 2B\kappa_1 w_1^a |h_1^+| |\lambda_1^+ - \dot{y}_\alpha| \\
 &\quad + (\kappa_1 A_{W_1^+} + M) (w_1^m |K_{21} h_1^+| |\lambda_1^- - \dot{y}_\alpha| - w_1^a |h_1^+| |\lambda_1^+ - \dot{y}_\alpha|) \\
 &\quad + 2B\kappa_1 w_4^a |h_4^-| (\lambda_4^+ - \dot{y}_\alpha) - 2B\kappa_1 w_4^m |h_4^-| (\lambda_4^- - \dot{y}_\alpha) \\
 &\quad + 2B\kappa_1 (-w_1^m |K_{21} h_1^+| + 2w_1^m |K_{21} h_1^+|) |\lambda_1^- - \dot{y}_\alpha| - 2B\kappa_1 w_1^a |h_1^+| |\lambda_1^+ - \dot{y}_\alpha| \\
 &\quad + (\kappa_1 A_{W_4^+} + M) w_4^a |h_4^+| (\lambda_4^+ - \dot{y}_\alpha) - (\kappa_1 A_{W_4^+} + M) w_4^m |h_4^-| (\lambda_4^- - \dot{y}_\alpha) \\
 &\quad + \mathcal{O}(1)B \left(2\vartheta + 2 \sum_{i \neq \{2,3\}} |q_i^+| + (|q_2^+| + |q_3^+|) \right) \\
 &\leq 0,
 \end{aligned}$$

which yields (4.10).

Case 4: *Close to the Lipschitz wall boundary.* This case differs from the Cauchy problem. Here we will use the particular property of the boundary condition (1.8): The flows of U and V are tangent to the Lipschitz wall, implying that they must be parallel with each other along the boundary. Then a piecewise constant weak solution is constructed only along the Hugoniot curves determined by the Riemann data $U(b)$ and $V(b)$, the states of solutions U and V , respectively, close to the boundary.

Proposition 5.2. *Suppose that $U(b) = (\check{u}, \check{v}, \check{p}, \check{\rho})$ and $V(b) = (\tilde{u}, \tilde{v}, \tilde{p}, \tilde{\rho})$ are states in a small neighborhood $O_\varepsilon(U_-)$ of U_- satisfying $\frac{\check{v}}{\check{u}} = \frac{\tilde{v}}{\tilde{u}} = \dot{z}_b$, and $\check{v}, \tilde{v} \approx 0$. Denote by $h_j(b)$ the strength of the j^{th} shock in the Riemann problem determined by $U(b)$ and $V(b)$, and by λ_j the corresponding j^{th} -characteristic speed. Then*

$$|\lambda_j - \dot{z}_b| \sim |h_1(b)|, \quad j = 2, 3, \quad (5.8)$$

$$|h_4(b)| \leq |h_1(b)| + \mathcal{O}(1)|h_2(b)||\lambda_2 - \dot{z}_b| + |h_1(b)|\mathcal{O}(1)|\dot{z}_b|, \quad (5.9)$$

$$|h_1(b)| = \bar{\mathcal{O}}(1)|h_4(b)|, \quad \frac{1}{2} < \bar{\mathcal{O}}(1) < \frac{3}{2}, \quad (5.10)$$

where \dot{z}_b is the slope of the Lipschitz wall.

Proof. We do the proof by analyzing the following two cases.

Case 1: $h_1(b) = 0$ and $h_4(b) = 0$ that corresponds to the case $\check{p} = \tilde{p}$. Starting at the state U_b , we move along the Hugoniot curves of the second and third families to reach V_b . Note that these two families are the contact Hugoniot curves, and so λ_2 and λ_3 are constant along the Hugoniot curves.

Given that $\lambda_{2,3} = \frac{v}{u}$, $\mathbf{r}_2 = (1, \frac{v}{u}, 0, 0)^\top$, and $\mathbf{r}_3 = (0, 0, 0, \rho)^\top$, the quantity $\frac{v}{u}$ remains unchanged as the initial value $\frac{v(U_b)}{u(U_b)}$, i.e., \dot{z}_b in this process by the boundary condition (1.8). Therefore, we conclude that $\lambda_{2,3} = \dot{z}_b$, equivalently,

$$\dot{z}_b - \lambda_{2,3} = 0.$$

Case 2: $h_1(b) \neq 0$ that corresponds to $\check{p} \neq \tilde{p}$. Starting at the state $U(b)$, we move along the 1-Hugoniot curve to reach U_1 , then possibly move along the 2-contact Hugoniot curve to reach U_2 , the 3-Hugoniot curve to reach U_3 , and the 4-Hugoniot curve to reach $V(b)$.

To make clear some essential relations among the strengths $h_1(b), h_2(b), h_3(b)$, and $h_4(b)$, we project (u, v, p, ρ) onto the (u, v) -plane. Let $\mathbf{r}_1|_u$ be the projection of \mathbf{r}_1 onto the u -axis, $\mathbf{r}_2|_{(u,v)}$ be the projection of \mathbf{r}_2 onto the (u, v) -plane; and so on. At the background state U_- , there holds

$$\begin{aligned} \mathbf{r}_1|_u &= -\mathbf{r}_4|_u, & \mathbf{r}_1|_v &= \mathbf{r}_4|_v, & \mathbf{r}_1|_{(p,\rho)} &= -\mathbf{r}_4|_{(p,\rho)}, \\ \mathbf{r}_2 &= \mathbf{r}_2|_{(u,v)}, & \mathbf{r}_3|_{(u,v)} &= 0. \end{aligned}$$

We first note that $h_4(b) \neq 0$. Given that $\mathbf{r}_1|_{(u,v)} = k_1(-\lambda_1, 1)^\top$ along with finite characteristic speeds λ_1 and $\dot{z}_b \approx 0$, there always holds $\dot{z}_b < -\frac{1}{\lambda_1}$ near the state U_- . So we can conclude that, in the (u, v) -plane, the derivative $\frac{dv}{du}$ along the 1-curve is always larger than \dot{z}_b . This implies that $\frac{v(U_1)}{u(U_1)} \neq \frac{v(U_b)}{u(U_b)}$. Meanwhile, we have $\frac{v(U_1)}{u(U_1)} = \frac{v(U_2)}{u(U_2)} = \frac{v(U_3)}{u(U_3)}$ and $\frac{v(V_b)}{u(V_b)} = \frac{v(U_b)}{u(U_b)}$. Hence,

$$\frac{v(U_1)}{u(U_1)} = \frac{v(U_2)}{u(U_2)} = \frac{v(U_3)}{u(U_3)} \neq \frac{v(V_b)}{u(V_b)}.$$

Thus, we conclude that there is some distance along the 4-Hugoniot curve to reach V_b . Therefore, $h_4 \neq 0$.

Next, we present an essential estimate to bound $|h_4|$ more precisely in terms of $|h_1|$. To that end, define the signed length of $(U_1 - U_b)|_{(u,v)}$ and $(V_b - U_3)|_{(u,v)}$ by d_1 and d_4 on the (u, v) -plane:

$$d_1 = \begin{cases} \|(U_1 - U_b)|_{(u,v)}\| & \text{if } h_1 > 0, \\ -\|(U_1 - U_b)|_{(u,v)}\| & \text{if } h_1 < 0, \end{cases}$$

and

$$d_4 = \begin{cases} \|(V_b - U_3)|_{(u,v)}\| & \text{if } h_4 > 0, \\ -\|(V_b - U_3)|_{(u,v)}\| & \text{if } h_4 < 0. \end{cases}$$

Secondly, we note that

$$|\lambda_2 - \dot{z}_b| = \mathcal{O}(1)|d_1| = \mathcal{O}(1)|h_1(b)|.$$

Moreover, since $\lambda_2 = \frac{v(U_1)}{u(U_1)} = \frac{v(U_2)}{u(U_2)} = \lambda_3$, we can similarly conclude

$$|\lambda_3 - \dot{z}_b| = \mathcal{O}(1)|d_1| = \mathcal{O}(1)|h_1(b)|.$$

Using the following projections on the (u, v) -plane,

$$\begin{aligned} \mathbf{r}_1|_u &= -\mathbf{r}_4|_u, & \mathbf{r}_1|_v &= \mathbf{r}_4|_v, \\ \mathbf{r}_2 &= \mathbf{r}_2|_{(u,v)}, & \mathbf{r}_3|_{(u,v)} &= 0. \end{aligned}$$

Thirdly, we note that

$$-d_4 = \mathcal{O}(1)h_2(b)(\lambda_2 - \dot{z}_b) + \tilde{d},$$

where $\tilde{d} \cos \varphi_1 = d_1 \cos \varphi_2$, φ_1 denotes the angle between $(1, \dot{z}_b)$ and $\mathbf{r}_4|_{(u,v)}$, φ_2 denotes the angle between $\mathbf{r}_1|_{(u,v)}$ and $(1, \dot{z}_b)$, $\varphi_1 = \varphi_2 + 2\alpha$ for $\alpha = \arctan(\dot{z}_b)$, and

$$\begin{aligned} \tilde{d} &= d_1 \frac{\cos \varphi_2}{\cos \varphi_1} = d_1 \frac{\cos(\varphi_1 - 2\alpha)}{\cos \varphi_1} = d_1 \frac{\cos \varphi_1 \cos(2\alpha) + \sin \varphi_1 \sin(2\alpha)}{\cos \varphi_1} \\ &= d_1 (\cos(2\alpha) + \mathcal{O}(1)\sin(2\alpha)) = d_1 (1 + \mathcal{O}(1)\alpha) = d_1 (1 + \mathcal{O}(1)\dot{z}_b). \end{aligned}$$

Hence, there holds

$$-d_4 = \mathcal{O}(1)h_2(b)(\lambda_2 - \dot{z}_b) + d_1(1 + \mathcal{O}(1)\dot{z}_b).$$

At U_- , there also holds $\mathbf{r}_1|_{(u,p,\rho)} = -\mathbf{r}_4|_{(u,p,\rho)}$ and $\mathbf{r}_1|_v = \mathbf{r}_4|_v$, which implies

$$\frac{d_1}{h_1} = \frac{d_4}{h_4}.$$

Hence we note the following key estimate:

$$-h_4(b) = \mathcal{O}(1)h_2(b)(\lambda_2 - \dot{z}_b) + h_1(b)(1 + \mathcal{O}(1)\dot{z}_b). \quad (5.11)$$

Estimate (5.11) now implies

$$\begin{aligned} |h_4(b)| &\leq |h_1(b)| + \mathcal{O}(1)|h_2(b)||\lambda_2 - \dot{z}_b| + |h_1(b)|\mathcal{O}(1)|\dot{z}_b| \\ &\leq |h_1(b)| + \mathcal{O}(1)(|h_2(b)| + |\dot{z}_b|)|h_1(b)|, \end{aligned}$$

yielding

$$|h_1(b)| = \tilde{\mathcal{O}}(1)|h_4(b)| \quad \text{with } \frac{1}{2} < \tilde{\mathcal{O}}(1) < \frac{3}{2},$$

given that $|h_2(b)| + |\dot{z}_b|$ is always small enough, and this is guaranteed by the sufficiently small total variation of the initial perturbation \widetilde{U}_0 and the perturbation of the boundary. \square

We note that the requirement $\frac{\bar{v}}{u} = \frac{\hat{v}}{u} = \dot{z}_b$ in Proposition 5.2 is just the boundary condition (1.8) because \dot{z}_b here is the slope of the Lipschitz wall.

Applying Proposition 5.2 now yields

$$\begin{aligned} E_{b,1} &= |q_1(b)|W_1(b)(\dot{z}_b + \lambda_1) \\ &= -4B\kappa_1w_1^b|h_1(b)||\lambda_1| + \mathcal{O}(1)|h_1(b)| \\ &= -4B\kappa_1w_1^b|h_1(b)||\lambda_1| + \mathcal{O}(1)|h_4(b)|, \\ E_{b,j} &= |q_j(b)|W_j(b)(\dot{z}_b + \lambda_j) = |q_j(b)|W_j(b)(\dot{z}_b - \lambda_j) + 2\lambda_j|q_j(b)|W_j(b) \\ &= \mathcal{O}(1)w_j^b|h_j(b)|(\dot{z}_b - \lambda_j) + \mathcal{O}(1)\lambda_jw_j^b|h_j(b)| \\ &= \mathcal{O}(1)h_1(b) = \mathcal{O}(1)h_4(b), \quad j = 2, 3, \\ E_{b,4} &= |q_4(b)|W_4(b)(\dot{z}_b + \lambda_4) \\ &= 4B\kappa_1w_4^b|h_4(b)||\lambda_1| + \mathcal{O}(1)|h_4(b)| \\ &\leq 4B\kappa_1|\lambda_1|w_4^b(|h_1(b)| + \mathcal{O}(1)|h_2(b)||\lambda_2 - \dot{z}_b| + \mathcal{O}(1)|h_1(b)||\dot{z}_b|) + \mathcal{O}(1)|h_4(b)|. \end{aligned} \quad (5.12)$$

Using Lemma 5.1, we can choose w_1^b and w_4^b such that

$$w_4^b < w_1^b.$$

Then, with the total variation of the incoming flow perturbation and the boundary perturbation small enough and κ_1 large enough, one has

$$\begin{aligned} \sum_{j=1}^4 E_{b,j} &= 4B\kappa_1(w_4^b - w_1^b)|h_1(b)||\lambda_1| \\ &\quad + \mathcal{O}(1)B\kappa_1|\lambda_1|h_4^b(|h_2(b)| + |\dot{z}_b|)|h_1(b)| + \mathcal{O}(1)|h_4(b)| \\ &\leq \tilde{\mathcal{O}}(1)4B\kappa_1(w_4^b - w_1^b)|h_4(b)||\lambda_1| \\ &\quad + \mathcal{O}(1)B\kappa_1|\lambda_1|w_4^b(|h_2(b)| + |\dot{z}_b|)|h_1(b)| + \mathcal{O}(1)|h_4(b)| \leq 0, \end{aligned}$$

provided that $|h_2(b)| + |\dot{z}_b|$ is sufficiently small. This is guaranteed since the total variation of the incoming flow perturbation and the boundary perturbation are sufficiently small.

6. EXISTENCE OF A SEMIGROUP OF SOLUTIONS

As a corollary of the essential estimates in Sections 3–5, we can now establish the existence of the semigroup \mathcal{S} generated by the wave-front tracking method, as well as the Lipschitz continuity of \mathcal{S} .

Proposition 6.1. *Suppose that $TV(\widetilde{U}_0(\cdot)) + TV(g'(\cdot))$ is small enough. Then the map*

$$(\overline{U}(\cdot), x) \mapsto U^\vartheta(x, \cdot) := \mathcal{S}_x^\vartheta(\overline{U}(\cdot))$$

produced by the wave-front tracking algorithm is a uniformly Lipschitz continuous semigroup satisfying the properties:

- (i) $\mathcal{S}_0^\vartheta \overline{U} = \overline{U}$, $\mathcal{S}_{x_1}^\vartheta \mathcal{S}_{x_2}^\vartheta \overline{U} = \mathcal{S}_{x_1+x_2}^\vartheta \overline{U}$, for all $x_1, x_2 \geq 0$;
- (ii) $\|\mathcal{S}_x^\vartheta \overline{U} - \mathcal{S}_x^\vartheta \overline{V}\|_{L^1} \leq C\|\overline{U} - \overline{V}\|_{L^1} + C\vartheta x$, for all $x \geq 0$.

Proof. Since \mathcal{S}^ϑ is generated by the wave-front tracking algorithm, property (i) is immediate. Next, property (ii) is proved as follows. Take a pair of front tracking ϑ -approximate solutions U^ϑ and V^ϑ of (1.1) and (1.7)–(1.8) with $\overline{U}(\cdot)$ and $\overline{V}(\cdot)$ as the initial data, respectively. Using (4.5) and (4.15), at any $x \geq 0$, we have

$$\begin{aligned} \|U^\vartheta(x) - V^\vartheta(x)\|_{L^1} &\leq C\Phi(U^\vartheta(x), V^\vartheta(x)) \\ &\leq C\Phi(U^\vartheta(0), V^\vartheta(0)) + C\nu x \\ &\leq C\|\overline{U} - \overline{V}\|_{L^1} + C\vartheta x. \end{aligned}$$

Hence, the ϑ -semigroup is Lipschitz continuous.

Definition 6.1. For a given $\nu_0 > 0$, we define the domain:

$$\mathcal{D} = cl \left\{ \begin{array}{l} \text{the set consisting of points } U : \mathbb{R} \mapsto \mathbb{R}^4 \\ \text{such that there exists one point } y^i \in \mathbb{R} \text{ and} \\ \tilde{U}(y) = \begin{cases} U_-, & g(x) \leq y \leq y^i, \\ U_+, & y^i < y, \end{cases} \\ \text{so that } U - \tilde{U} \in L^1(\mathbb{R}; \mathbb{R}^4) \text{ and } TV(U - \tilde{U}) \leq \nu_0. \end{array} \right.$$

Remark 6.1. Given a solution $U(x, y)$ to the initial-boundary value problem of (1.1) and (1.7)–(1.8), we note that, if $U^x(y) := U(x, y) \in \mathcal{D}$ at any fixed $x \geq 0$, then $y^i > g(0) = 0$ at $x = 0$ and $y^i > g(x)$ for $x > 0$ as a strong vortex sheet/entropy wave is present.

The semigroup \mathcal{S} generated by the wave-front tracking algorithm is provided by the next theorem.

Theorem 6.1. *Suppose that $TV(\widetilde{U}_0(\cdot)) + TV(g'(\cdot))$ is small enough. Then, in the L^1 -norm, \mathcal{S}^ϑ produced by the wave-front tracking algorithm is a Cauchy sequence. Denote this unique limit by \mathcal{S} such that, for any $x > 0$, $\mathcal{S}_x(\overline{U}) = \lim_{\vartheta \rightarrow 0} \mathcal{S}_x^\vartheta(\overline{U})$. Then the map $\mathcal{S} : [0, \infty) \times \mathcal{D} \mapsto \mathcal{D}$ is a uniformly Lipschitz semigroup in L^1 . In particular, the entropy solution to the initial-boundary problem (1.1) and (1.7)–(1.8) constructed by the wave-front tracking algorithm is unique and L^1 stable.*

Based on the essential estimates in Sections 3–5, the proof of Theorem 6.1 can be shown in the same way as the argument given in [6]. Also see Chen-Li [9].

7. UNIQUENESS OF ENTROPY SOLUTIONS IN THE VISCOSITY CLASS

In this section, as an immediate consequence of the estimates obtained in Sections 4–6, we find that the semigroup \mathcal{S} produced by the wave-front tracking method is the only *standard Riemann semigroup* (SRS) in the sense of Definition 7.1 given below. In other words, the semigroup defined by the wave-front tracking method is the canonical trajectory of the standard Riemann semigroup (SRS). This yields the uniqueness of entropy solutions in a broader class of viscosity solutions as introduced by Bressan in [4]. Furthermore, it coincides with the semigroup trajectory generated by the wave-front tracking method.

Definition 7.1. Problem (1.1) and (1.7)–(1.8) is said to have a standard Riemann semigroup (SRS) if, for some small ν_0 , there exist a continuous mapping $\mathcal{R} : [0, \infty) \times \mathcal{D} \mapsto \mathcal{D}$ and a constant L satisfying the following properties:

- (i) (*Semigroup property*): $\mathcal{R}_0 \bar{U} = \bar{U}$, $\mathcal{R}_{x_1} \mathcal{R}_{x_2} \bar{U} = \mathcal{R}_{x_1+x_2} \bar{U}$;
- (ii) (*Lipschitz continuity*): $\|\mathcal{R}_x \bar{U} - \mathcal{R}_x \bar{V}\|_{L^1} \leq L \|\bar{U} - \bar{V}\|_{L^1}$;
- (iii) (*Consistency with the Riemann solver*): Given piecewise constant initial data $\bar{U} \in \mathcal{D}$, then, for all $x \in [0, \nu_0]$, the function $U(x, \cdot) = \mathcal{S}_x \bar{U}$ coincides with the solution of (1.1) and (1.7)–(1.8) obtained by piecing together the standard Riemann solutions and the lateral Riemann solutions.

Following the argument in [4], we employ the estimates obtained in Sections 4–6 to conclude

Theorem 7.1. *Suppose that problem (1.1) and (1.7)–(1.8) has a standard Riemann semigroup $\mathcal{R} : [0, \infty) \times \mathcal{D} \mapsto \mathcal{D}$. Consider the semigroup \mathcal{S} produced by the wave-front tracking method, that is, $\mathcal{S}_x(\bar{U}) = \lim_{\vartheta \rightarrow 0} \mathcal{S}_x^\vartheta(\bar{U})$. Assume $\bar{U} \in \mathcal{D}$. Then, for all $x > 0$, $\mathcal{R}_x \bar{U} = \mathcal{S}_x \bar{U}$. Furthermore, a continuous map $U : [0, X] \mapsto \mathcal{D}$ is a viscosity solution of problem (1.1) and (1.7)–(1.8) defined in [4] if and only if*

$$U(x, \cdot) = \mathcal{R}_x \bar{U} \quad \text{for any } x \in [0, T]. \tag{7.1}$$

In particular, a continuous map $U : [0, X] \mapsto \mathcal{D}$ is a viscosity solution if and only if

$$U(x, \cdot) = \mathcal{S}_x \bar{U} \quad \text{for any } x \in [0, T]. \tag{7.2}$$

The proof here follows a similar argument to the one presented in [4]. The only difference is that there is a strong vortex sheets/entropy waves in our problem. Nonetheless, one can proceed with the proof by considering the convergence of the wave-front tracking method which is shown in Section 3.

Remark 7.1. In the simpler cases of the isentropic or isothermal Euler flow (1.5), as well as the potential flow, as far as the L^1 -stability problem is of concern, we realize the same results as for the full Euler system (1.1).

Acknowledgements: The research of Gui-Qiang Chen was supported in part by the National Science Foundation under Grants DMS-0935967 and DMS-0807551, the UK EPSRC Science and Innovation Award to the Oxford Centre for Nonlinear PDE (EP/E035027/1), the NSFC under a joint project Grant 10728101, and the Royal Society–Wolfson Research Merit Award (UK). The research of Vaibhav Kukreja was supported in part by the National Science Foundation under Grants DMS-0935967 and DMS-0807551, the UK EPSRC Science and Innovation Award to the Oxford Centre for Nonlinear PDE (EP/E035027/1).

REFERENCES

- [1] P. Baiti and K. Jenssen, On the front-tracking algorithm, *J. Math. Anal. Appl.* 217 (1998), 395–404.
- [2] S. Biachini and A. Bressan, Vanishing viscosity of nonlinear hyperbolic systems, *Ann. of Math.* 161 (1) (2005), 223–342.
- [3] A. Bressan, Global solutions of systems of conservation laws by wave-front tracking, *J. Math. Anal. Appl.* 170 (1992), 414–432.
- [4] A. Bressan, The unique limit of the Glimm scheme, *Arch. Ration. Mech. Anal.* 130 (1995), 205–230.
- [5] A. Bressan, *Hyperbolic Systems of Conservations Laws: The One-Dimensional Cauchy Problem*, Oxford Univ. Press, Oxford, 2000.
- [6] A. Bressan and R. M. Colombo, The semigroup of 2×2 conservation laws, *Indiana Univ. Math. J.* 44 (1995), 677–725.
- [7] A. Bressan, G. Crasta, and R. M. Colombo, Well-posedness of the Cauchy problem for $n \times n$ systems of conservation laws, *Mem. Amer. Math. Soc.* 146 (694), 2000.
- [8] A. Bressan, T.-P. Liu, and T. Yang, L^1 stability estimates for $n \times n$ conservation laws, *Arch. Ration. Mech. Anal.* 149 (1999), 1–22.

- [9] G.-Q. Chen and T.-H. Li, Well-posedness for two-dimensional steady supersonic Euler flows past a Lipschitz wedge, *J. Differential Equations*, 244 (2008), 1521–1550.
- [10] G.-Q. Chen, Y.-Q. Zhang, and D.-W. Zhu, Stability of compressible vortex sheets in steady supersonic Euler flows over Lipschitz walls, *SIAM J. Math. Anal.* 38 (2007), 1660–1693.
- [11] R. Courant and K. O. Friedrichs, *Supersonic Flow and Shock Waves*, Interscience, New York, 1948.
- [12] A. Corli and M. Sablé-Tougeron, Stability of contact discontinuities under perturbations of bounded variation, *Rend. Sem. Mat. Univ. Padova*, 97 (1997), 35–60.
- [13] C. M. Dafermos, Polygonal approximations of solutions of the initial value problem for a conservation law, *J. Math. Anal. Appl.* 38 (1972), 33–41.
- [14] C. M. Dafermos, *Hyperbolic Conservation Laws in Continuum Physics*, Second ed., Springer-Verlag, Berlin, 2005.
- [15] R. J. DiPerna, Global existence of solutions to nonlinear hyperbolic systems of conservation laws, *J. Differential Equations*, 20 (1976), 187–212.
- [16] J. Glimm, Solution in the large for nonlinear systems of conservation laws, *Comm. Pure Appl. Math.* 18 (1965), 697–715.
- [17] H. Holden and N. Risebro, *Front Tracking for Hyperbolic Conservation Laws*, Springer-Verlag, New York, 2002.
- [18] Ph. LeFloch, *Hyperbolic Systems of Conservation Laws: The Theory of Classical and Nonclassical Shock Waves*, Birkhäuser-Verlag, Basel, 2002.
- [19] M. Lewicka, L^1 stability of patterns of non-interacting large shock waves, *Indiana Univ. Math. J.* 49 (2000), 1515–1537.
- [20] M. Lewicka, Stability conditions for patterns of noninteracting large shock waves, *SIAM J. Math. Anal.* 32 (2001), 1094–1116.
- [21] M. Lewicka and K. Trivisa, On the L^1 well posedness of systems of conservation laws near solutions containing two large shocks, *J. Differential Equations*, 179 (2002), 133–177.
- [22] T.-P. Liu, The deterministic version of the Glimm scheme, *Comm. Math. Phys.* 57 (1977), 135–148.
- [23] T.-P. Liu and T. Yang, Well-posedness theory for hyperbolic conservation laws, *Comm. Pure Appl. Math.* 52 (1999), 1553–1586.
- [24] M. Sablé-Tougeron, Méthode de Glimm et problème mixte, *Ann. Inst. H. Poincaré Anal. Nonlinéaire*, 10 (1993), 423–443.

GUI-QIANG G. CHEN, MATHEMATICAL INSTITUTE, UNIVERSITY OF OXFORD, OXFORD, OX1 3LB, UK; DEPARTMENT OF MATHEMATICS, NORTHWESTERN UNIVERSITY, EVANSTON, IL 60208, USA; SCHOOL OF MATHEMATICAL SCIENCES, FUDAN UNIVERSITY, SHANGHAI 200433, CHINA

E-mail address: `chengq@maths.ox.ac.uk`

VAIBHAV KUKREJA, INSTITUTO DE MATEMÁTICA PURA E APLICADA (IMPA), RIO DE JANEIRO, BRAZIL; DEPARTMENT OF MATHEMATICS, NORTHWESTERN UNIVERSITY, EVANSTON, IL 60208, USA

E-mail address: `vaibhav@impa.br`; `vkukreja@math.northwestern.edu`